Spring 2010

Measurement of elastic modulus of PUNB bonded sand as a function of temperature

Jacob Andrew Thole
University of Iowa

MEASUREMENT OF ELASTIC MODULUS OF PUNB BONDED SAND AS A FUNCTION OF TEMPERATURE

by

Jacob Andrew Thole

A thesis submitted in partial fulfillment
of the requirements for the Master of
Science degree in Mechanical Engineering
in the Graduate College of
The University of Iowa

May 2010

Thesis Supervisor: Professor Christoph Beckermann

Graduate College
The University of Iowa
Iowa City, Iowa

CERTIFICATE OF APPROVAL

_____

MASTER'S THESIS

_____

This is to certify that the Master's thesis of

Jacob Andrew Thole

has been approved by the Examining Committee
for the thesis requirement for the Master of Science
degree in Mechanical Engineering at the May 2010 graduation.

Thesis Committee: _____
Christoph Beckermann, Thesis Supervisor

_____
Olesya Zhupanska

_____
Albert Ratner

ACKNOWLEDGMENTS

The author thanks Professor Christoph Beckermann for all his support and his unwavering expectations which guided me throughout. Special thanks are extended to Charlie Monroe, Alex Monroe, Antonio Melendez, Kent Carlson, Richard Hardin, and students of the solidification laboratory for their support and encouragement. Jerry Thiel and students at the University of Northern Iowa Metals Casting Center for their support with specimen production. Colby Swan and Rob Williams of the Civil Engineering Department at Iowa for their insight and generosity for allowing me to use their lab equipment. Finally, special thanks to the friends and family, especially William Monroe, Josh Vahle, and my parents Mary and Joel Thole, for all their support and understanding during the more difficult periods.

ABSTRACT

Foundries today use temporary molds made from silica sand with a resin bonding agent to hold a form until the metal is poured. With the aid of computer simulations, the molds are designed to produce good castings with minimal pattern iterations by calculating cooling and porosity. Stress analysis simulations are being developed using the current software, but the known mechanical properties for the sand mold are minimal and incomplete. This study measures the elastic modulus of bonded sand as a function of temperature to obtain baseline data for the model. Following ASTM standards, a three point bend test is used to measure the elastic modulus of chemically bonded sand as a function of temperature to better understand the complex nature of the mold as it undergoes heating and cooling. Multiple measurements of the elastic modulus of PUNB bonded silica sand are performed from room temperature to 500°C in a nitrogen atmosphere to capture the changes in the elastic modulus under heating. It is found that for an intermediate heating rate of 8°C/min, the elastic modulus decreases steeply from a room temperature value of about 3,600 MPa to 600 MPa at 125°C. Between 125°C and 250°C, the elastic modulus is relatively constant. Above 250°C, it increases to 1,200 MPa at 280°C and then decreases again to 800 MPa at 350°C. Above 350°C, the elastic modulus increases linearly with temperature until it reaches 2,200 MPa at 500°C. At approximately 500°C, the strength of the bonded sand vanishes. At a given temperature above 125°C, the elastic modulus can vary by more than a factor of two depending on the heating rate. Furthermore, the elastic modulus agrees with previous steady state temperature measurement literature when specimens are held at a constant temperature until the elastic modulus reach steady. It is also found that the addition of black iron oxide has no effect on the elastic modulus, whereas solvent removal before a test increases the stiffness of the bonded sand at temperatures below 150°C.

TABLE OF CONTENTS

LIST OF TABLES

Table

LIST OF FIGURES

Figure

CHAPTER 1. INTRODUCTION

Casting simulation software has recently made some progress in the area of prediction of stresses and distortion. However, significant gaps exist in the knowledge of the mechanical properties of the metal and mold materials. Monroe *et al*. [1] found that the predicted stresses and distortions in steel casting are particularly sensitive to the elastic modulus of the sand mold as shown in Figure 1. Monroe, having preliminary and incomplete data on the behavior of the mechanical properties of bonded sand, varied the elastic modulus of the bonded sand (Figure 1a) until the stress simulation agreed with experimental data (Figure 1b). The objective of the present study is to accurately measure the elastic modulus of phenolic urethane no-bake (PUNB) bonded sand as a function of temperature in order to provide improved input data for stress simulations.

Measurements of the elastic modulus are performed on PUNB bonded sand that is typical of steel casting molds. Using a three-point bend apparatus the specimens are tested inside an oven in an inert atmosphere under heating. The setup allows for elastic modulus measurements to be performed almost instantaneously. Hence, an almost continuous variation of the elastic modulus with temperature can be obtained. In particular, it is of interest to understand if the elastic modulus takes on the same values during cooling as during heating and if the original room temperature value is recovered at the completion of cooling. Another point of interest is if mold additives, such as black iron oxide, affect the elastic modulus.

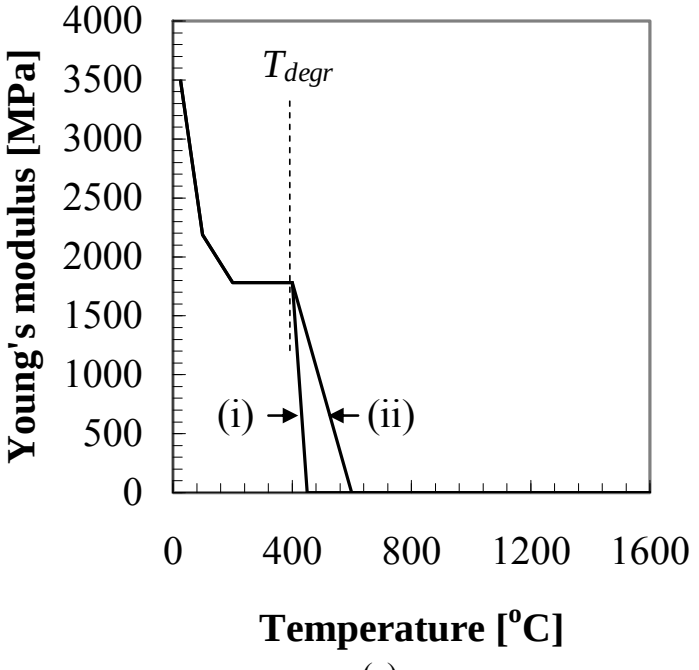

(a)

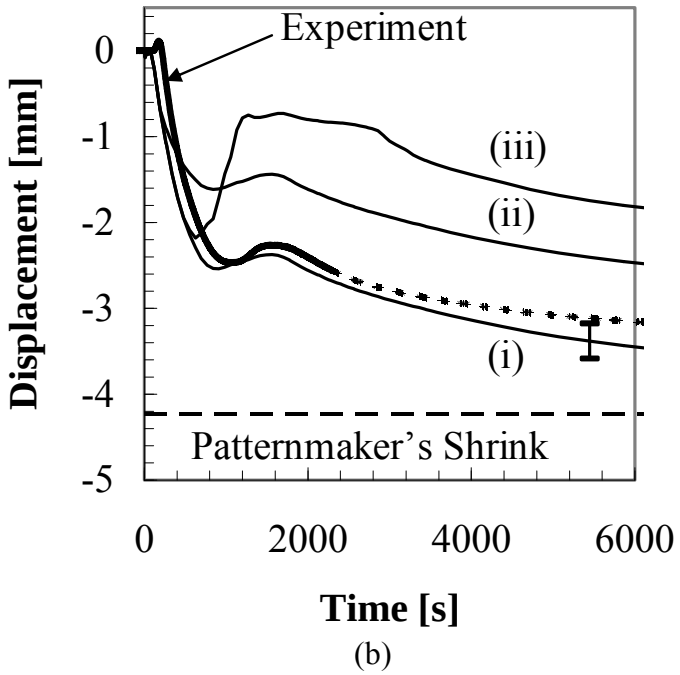

(b)

Figure 1: Effects of mechanical properties of bonded sand on stress analysis [1].
(a) Variation of elastic modulus of bonded sand temperature.
(b) Comparison of stress analysis for an unrestrained casting for three different cases: (i) baseline mold stiffness with degradation; (ii) higher mold stiffness at high temperatures with degradation; (iii) baseline mold stiffness without degradation.

CHAPTER 2. LITERATURE REVIEW

2.1 Phenolic Urethane Binder Systems

Though many different binder systems exist for the production of molds and cores, the foundry work horse is the phenolic urethane (PU) resin binder. This two part binder system containing a phenolformaldehyde resin (part 1) and an isocyanate resin (part 2) requires an amine catalyst to form the PU bond as described by Naro *et al*. [2] and Hoyt [3]. The difference between no-bake and coldbox is how the catalyst is introduced to the system. No-bake uses a liquid based catalyst usually introduced though a continuous mixer system where as coldbox uses a gaseous catalyst introduced after the sand coated with part 1 and 2 is blown into a core box [2]. Reference 2 also discusses mix ratios of part 1 to part 2 to minimize the amount of nitrogen present in the system as well as additives such as black iron oxide to help minimize the surface defects caused by nitrogen.

2.2 Elastic Modulus Data

Measurements of the elastic modulus of chemically bonded sand first appeared in the late 1950's, where the effects of grip, shape and gauge length of tensile test specimens were investigated by Wallace and coworkers [4]. In a later study [5] employing a strain gauge, they verified that approximately the same value for the elastic modulus at room temperature is obtained when measured under compressive, tensile or bending loading as can be seen in Figure 2. They report a room temperature elastic modulus for resin bonded sands to range from 3600 to 5800 MPa. It was found that for all loading methods, the bonded sand shows both elastic and brittle behavior. Another interesting feature is the ultimate strain for the compression specimen is approximately seven times higher than either the bending or tensile specimen.

In the early 80's Huang and Mobley [6] studied the mechanical properties of PUNB sand mixtures as a function of curing time. They report that after a cure time of 24

hours the room temperature elastic modulus approaches steady state. Figure 3 shows the results of their tests. The average fully cured room temperature elastic modulus is reported as 2654 MPa. Huang and Mobley also report the room temperature elastic modulus at 24 hours as a function of binder percentage, but reported binder percentages are higher than typical foundry practices for ferrous casting applications [2].

More recently, the elastic modulus of phenolic urethane cold-box (PUCB) bonded sand was measured at elevated steady-state temperatures using a three-point bend apparatus [7]. It was found in this study that the elastic modulus decreases from about 4,300 MPa at room temperature to 2,200 MPa at 200°C (Figure 4). Above 200°C, the elastic modulus was observed to remain constant, except for a temporary re-stiffening to 3,000 MPa at 300°C (Figure 4). At 400°C, another increase to 3,000 MPa was measured. Very recently, Thiel [8] performed elevated temperature elastic modulus measurements of chemically bonded sand using a tensile testing machine with an extensometer and an elongated dog-bone test specimen. The results, shown in Figure 5, were in approximate agreement with those of [6] and [7]. In both References [7] and [8], the bonded sand specimens were heated in an oven (in an inert atmosphere) to the desired test temperature, and the elastic modulus measurements were performed well after the specimens reached a uniform and constant temperature. The effect of heating rate was not investigated. In Reference [7], the measurements were performed inside of the oven, whereas in Reference [8] the specimens were removed from the oven before testing. In both references, the elastic modulus was measured at no more than ten discrete temperatures. Furthermore, the variation of the elastic modulus during cooling from an elevated temperature was not investigated.

2.3 Elastic Modulus Tests

Since the study requires tests to be performed at such high elevated temperatures standard stress-strain tests become much more complicated due to the sensitivity of the testing equipment.

Thiel [8] used a tensile testing machine with an extensometer clipped to the surface of an elongated dog-bone specimen. He overcame the issue of keeping temperature sensitive equipment cool by removing elevated temperature test specimens from the oven and performing tests at room temperature. In order to keep the specimen in a neutral elevated temperature atmosphere, the jaws of the extensometer would need to pass through a barrier into the heat affected zone while keeping the piezoelectric or strain-gage equipment outside the heat affected zone. Doing this will reduce the sensitivity of the extensometer.

A compression test using a similar system to Reference 8 could also be performed. The major advantage of a compression test is any plastic results would be valid for the majority of the stress field in a real casting.

Another slightly more complex method is a three or four point bend apparatus used by Reference 7. The advantage of using a three point over a four point bend apparatus is the simplicity of the fixture and easier adaptation to high temperature studies [9]. Reference 7 studied the results of both methods and found little variation between the two methods. A bend test is also more sensitive than compression or tensile tests since less force is required to obtain equivalent strains. This eliminates expensive hydraulic testing equipment necessary for compression and tension test loads. However, bend tests are more prone to error due to variations pointed out by Baratta [10].

Another promising but very complex method is the sonic excitation test method which uses flexural vibrations to measure the elastic modulus of beam specimens. Kline [11, 12] and Heybey *et al.* [13] report promising results for elastic modulus test measurements at elevated temperatures. Another promising feature of sonic excitation is

the minimal contact and stress induced to the specimen. Again, the major drawback to this method is the complexity and cost of the equipment necessary to perform the test.

2.4 Mold Temperature Simulation

The effect of different heating rates is of interest since real castings undergo different heating and cooling rates depending on the size of the casting and the distance from the casting surface. Figures 6 and 7 show the temperature results of a solidification simulation of a large 3 in thick steel casting section with a 3 in thick mold. It can be seen that within a distance of 1 in from the mold-metal interface, the temperatures in the mold reach values higher than 1,000°C (Figure 6) and the heating rates are above 50°C/min (Figure 7). Such high heating rates are difficult to achieve in an oven. In addition, a reasonably sized specimen would not be isothermal when heated at such high rates. However, at distances greater than 1 in from the mold-metal interface the heating rates are much lower, while the mold temperatures still reach values above 400°C. Between 1.5 in to 3 in from the mold-metal interface, the mold heating rates vary from about 20°C/min to 5°C/min. Heating rates of that order of magnitude are utilized in the present measurements. Figure 7 shows that after the initial heating, the mold cools down again. The cooling rates are much lower in magnitude than the heating rates. They decrease from about 1°C/min to 0.2°C/min with increasing distance from the mold-metal interface (Figure 7). During the time period when the temperatures in the mold decrease, the mold can still have a strong effect on casting distortion [1].

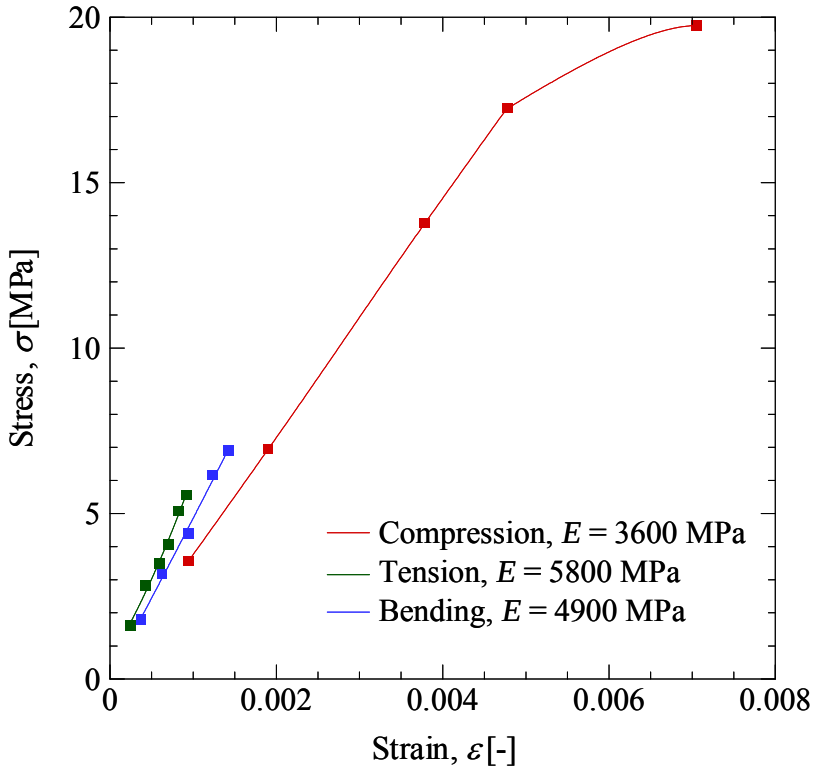

Figure 2: Room temperature stress-strain curves of resin bonded sand for three different loading methods [5].

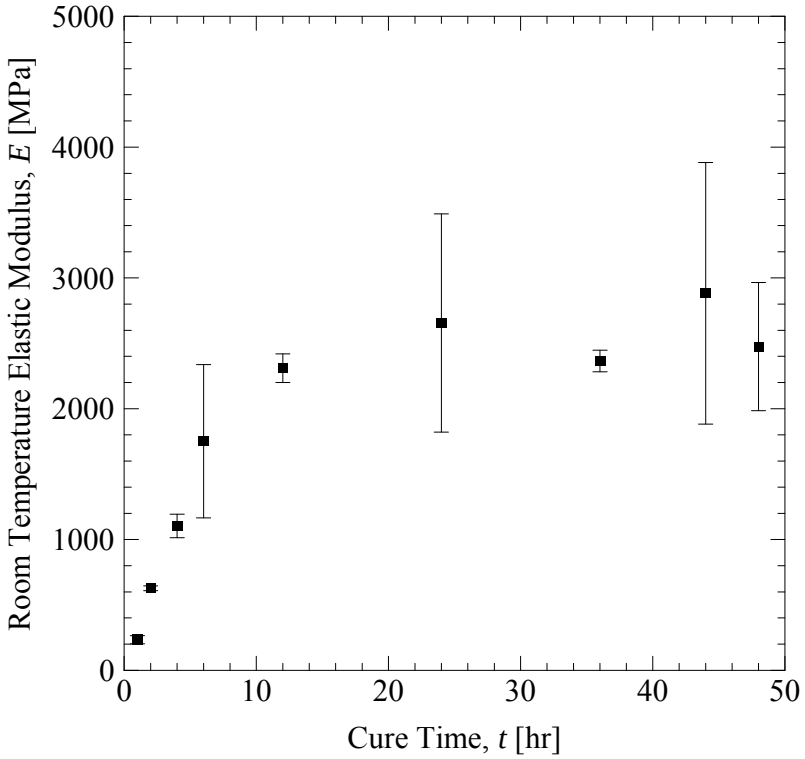

Figure 3: Room temperature elastic modulus as a function of curing time for a PUNB tensile test specimen [6].

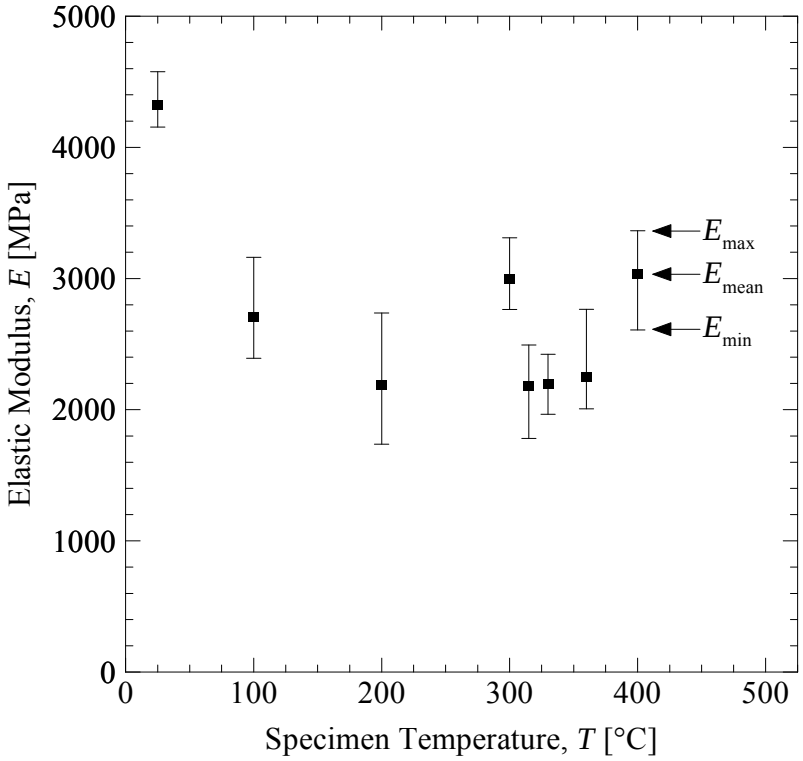

Figure 4: Elastic modulus for a cold box resin bonded sand as a function of temperature using a three-point bend test [7].

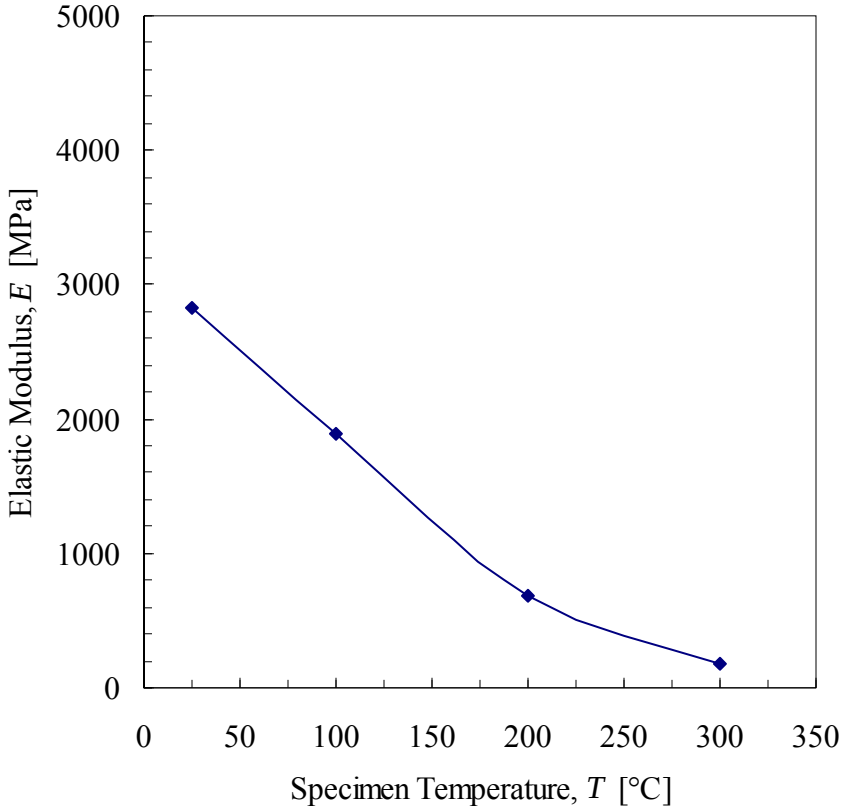

Figure 5: Elastic modulus for a cold box resin bonded sand as a function of temperature using a tensile testing machine with an extensometer [8].

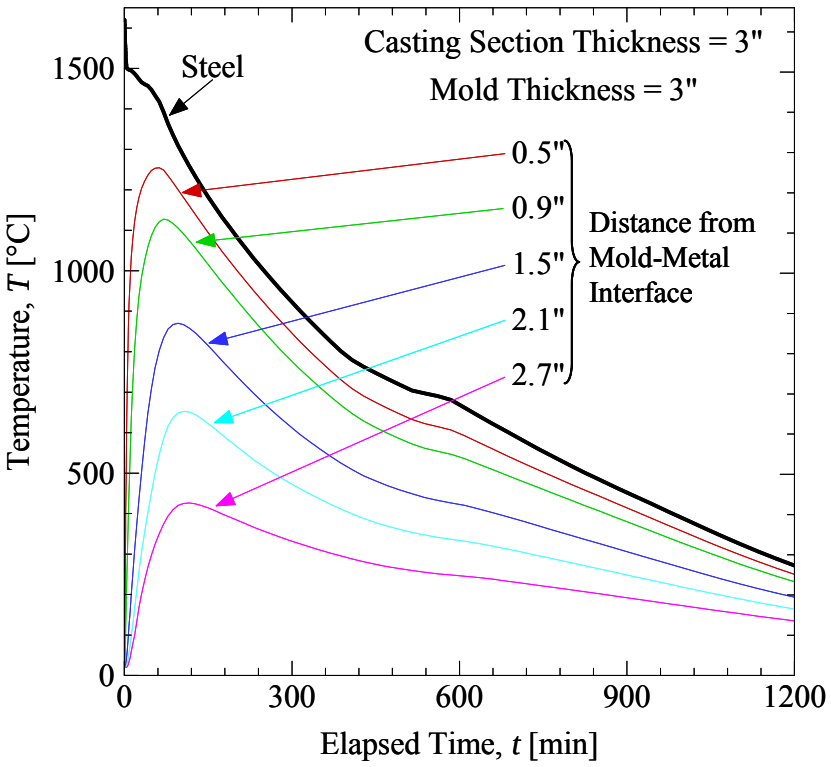

Figure 6: Predicted temperatures during casting of a three inch thick steel section surrounded by a three inch thick sand mold.

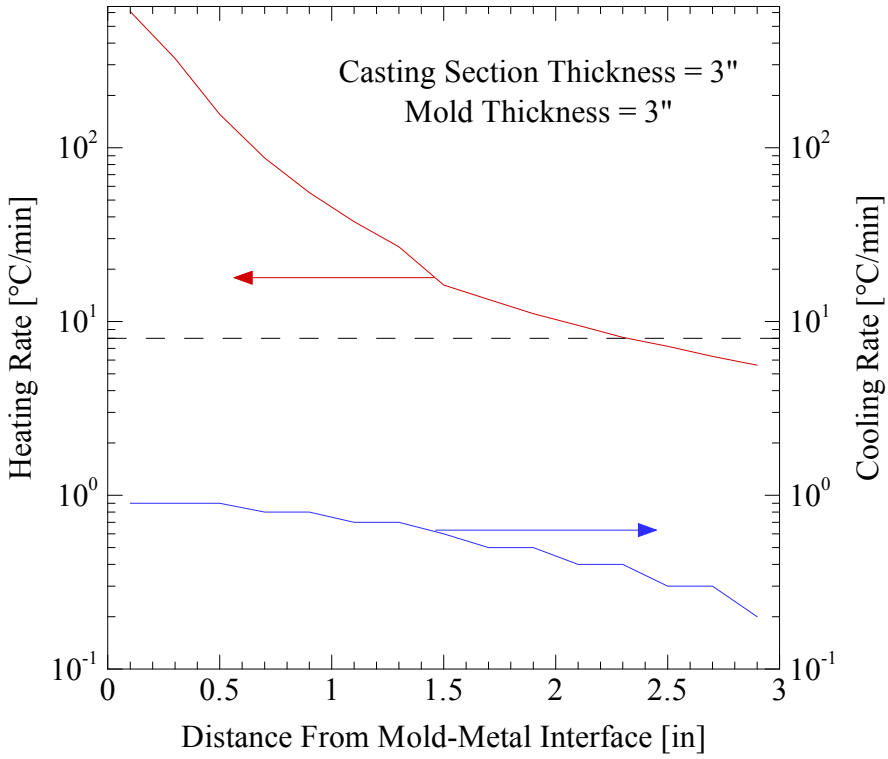

Figure 7: Predicted heating/cooling rates during casting of a three inch thick steel section surrounded by a three inch thick sand mold.

CHAPTER 3. EXPERIMENTS

The following sub-sections describe the preparation of the test specimens and the design of the experimental setup. Then, a brief validation of the present tests is presented in which the elastic modulus of ASTM 304 stainless steel is measured at room and elevated temperatures. Finally an error analysis is presented.

3.1 Specimen Preparation

The test specimens were prepared from silica lake sand with a grain fineness number of 55 (IC55) and a phenolic urethane no-bake (PUNB) binder system with black iron oxide (BIO). The grain fineness number is used as a gauge to determine relative size of the sand grain but does not guarantee a normal distribution or uniform spread in grain size when compared to other sands of the same GFN. A #20 sieve has a 850 micron mesh opening where a #70 has a 212 micron opening. Reference 2 states that subangular lake silica sand with a GFN of 50 to 70 is commonly used for most foundry practices. As shown in Figure 8, a nine screen test was run to verify the grain fineness number and measure the size distribution of the sand grains. Other specimen characteristics are summarized in Table 1. The values for the binder percentage, binder ratio, catalyst percentage and additives were obtained by polling seven steel foundries and taking the average of their responses. The porosity of the specimens was measured using a standard immersion test.

The specimens were prepared by first mixing the black iron oxide into the sand using a kitchen-aid mixer to ensure a uniform distribution. Then, the binder was added according to a procedure recommended by the binder manufacturer. Part 1 and the catalyst were added to the sand, mixed for 45 seconds, and then tossed to bring the sand from the bottom to the top. The batch was mixed for another 45 seconds and tossed again. After the second toss, part 2 was added to the batch and mixed for another 45 seconds, which was followed by a third and final toss. The batch was mixed for a final 45 seconds

before depositing it into the dump box. The sand-binder mixture was then rammed by hand into the pattern, while striving to achieve a uniform density, and allowed to set in the pattern before stripping. The specimens were stripped when the compacted sand withstood 20 psi of compressive stress without visible deformation [2]. The dump box was capable of making six specimens with a 25.4 mm (1 in) square cross-section and a 228.8 mm (9 in) length. The specimens were allowed to cure for at least 24 hours before testing [6]. A photograph of a test specimen is shown in Figure 9.

3.2 Experimental Setup

A schematic of the three-point bend apparatus is shown in Figure 10. Photographs of various aspects of the experimental setup are provided in Figure 11 to Figure 13. The three-point bend apparatus was placed inside a model OH-O1O-F1_CO-12-12-18 Thermcraft oven capable of reaching 538°C (1,000°F) (Figure 11). The oven was purged of oxygen using nitrogen from a tank at a flow rate of 1 m^3/hr (35 ft^3/hr). The temperature of the oven was controlled using a 2216 Eurotherm model 1D1-16-230 control system. This system controls the temperature using a 230V, 3000W heating coil at 14.6 Amps. A cooling system, consisting of copper tubing through which cold water was circulated, was added to the oven to cool the system after a test at elevated temperature. The use of a separate cooling system allows the specimen to cool in an oxygen-free environment over a range of cooling rates.

The three-point bend test fixture was designed to follow ASTM Standard D5934 [14], a method for measuring the elastic modulus of thermoplastics and thermosetting plastics. The support and loading heads were made from 12.54 mm (0.5 in) diameter cylindrical steel bars. The bars provide enough surface area to prevent any indentation caused by the loading or support heads. The support heads were welded to a base plate to ensure a constant support span of 190.56 mm (7.5 in) (Figure 12). This distance between the supports results in an overhang of the specimens that is sufficient to avoid slipping.

The loading head was aligned using a guide that was welded to the base plate (Figure 12). The guide ensures consistent placement of the loading head in order to reduce variability in the elastic modulus measurements.

Specimen deflection was measured using two Omega LD610-5 linear variable differential transformers (LVDTs). The LVDTs were located outside the oven by suspending them from a ladder stand (Figure 11). Glass silica rods were used to extend the LVDT probes into the oven through a port hole located above the fixture. The port hole was insulated with fiberglass to protect the LVDTs from the oven when operated at high temperatures. One probe was situated on a table that straddles the specimen and rests on the support heads (Figure 12). This LVDT measured the displacement of the support heads. The loading head probe passed through a hole in the table and a tube that was welded to a small plate which, in turn, was placed on the loading head (Figure 12). This prevents the loading head probe from "walking" off the loading head and rendering the test invalid.

The specimen was loaded using a cantilever system located beneath the oven (Figure 13). The loading head was connected to the cantilever system using a series of mechanical connections exiting the oven through a port hole located directly beneath the test fixture. Between the port hole and the cantilever system, a load cell (Omega LC703-50) was installed to measure the applied force. The cantilever system consisted of a wooden board that was connected by a hinge to the table on which the oven rested. A hanging mass at the opposite end of the hinge provided the loading force for the system. The load was controlled with an eye and hook turnbuckle that supported the cantilever (Figure 13). Using a simple wrench, the load could be increased and decreased in a rapid fashion.

Two Type K thermocouples were used to measure the surface and center temperature of a separate "dummy" specimen located at the same elevation in the oven as

the test specimen. A dummy specimen was used in order to keep the test specimen free of any modifications.

All devices were powered using an Elenco Precision Deluxe model XP-620 regulated power supply. The data was collected using a 16-bit IOtech 3005 Personal DAQ system connected to a laptop via USB. The software DasyLab was used to control the data acquisition system. A sampling frequency of 10 Hz, with an over-sampling rate of 8192, was used for all measurements. With these settings, each analog channel is sampled for 8,192 μs and a 16-bit average value over the scan period is returned.

The specimen deflection, D, was obtained by taking the difference between the displacements measured by the loading head and support head displacement LVDTs. The load cell was carefully calibrated to measure the loading force, F. With this data, the stress σ, strain ε, and elastic modulus E, were calculated from the following three-point bend equations [14]:

$$\sigma = \frac{3FL}{2bd^2} \tag{1}$$

and

$$\varepsilon = \frac{6Dd}{L^2} \tag{2}$$

thus

$$E = \frac{\sigma}{\varepsilon} = \frac{L^3}{4bd^3}\left(\frac{F}{D}\right) \tag{3}$$

where L is the support span, b is the specimen width as viewed by the loading head, and d is the specimen depth as viewed by the loading head.

3.3 Validation

In order to validate the present experimental setup and measurement procedures, at both room temperature and elevated temperatures, tests were performed using a

material with a well-known elastic modulus. The material chosen was ASTM 304 stainless steel. Figure 14 compares the present elastic modulus measurements with the measurements of Sakumoto *et al.* [15]. Good agreement can be observed at both room temperature and 400°C.

3.4 Error Analysis

A simple root-sum-squares (RSS) error analysis was performed to estimate the error in the present elastic modulus measurements. Table 2 shows the sources of error in the individual measurements for a room temperature example. For the specimen deflection and the loading force, only the largest measured values (in the elastic regime) are listed. Table 3 shows the resulting ranges and errors in the elastic modulus. It can be seen that the measurement of the specimen deflection is the single largest source of error. The specimen width measurement is also a relatively large source of error, which can be attributed to the roughness of the top surface of the bonded sand specimens. Width and depth measurement errors were kept to a minimum by marking the mid point of the length with a marker for consistent measurements. Overall, the error in the present room temperature elastic modulus measurement is estimated to be ±1.5%. A similar accuracy can be expected at elevated temperatures.

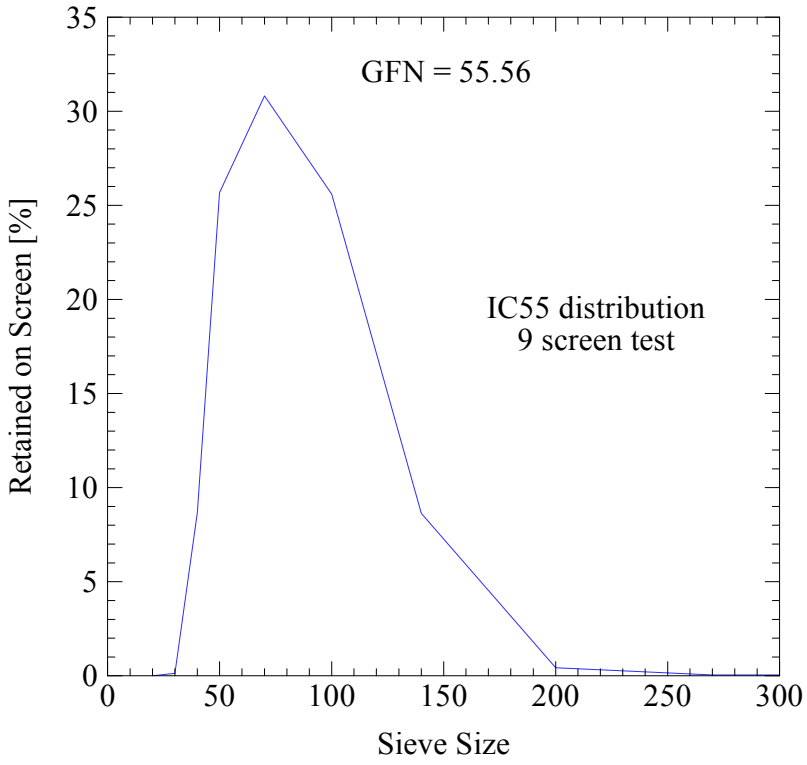

Figure 8: Nine screen sieve test performed on a 50 gram sample of IC55 silica lake sand, mean grain size is approximately 212 microns.

Table 1: Characteristics of the PUNB bonded sand specimens used in the elastic modulus measurements.

Sand Type	IC55 round grain silica lake sand
Binder	Pepset x1000, x2000
Catalyst	Pepset 3500
Binder Percentage	1.25% by total weight
Binder Ratio	60:40
Catalyst Percentage	8% of binder weight
Additives	3% black iron oxide by total weight
Specimen Porosity, $\bar{\phi} \pm 1\sigma$ [%]	32.8 ± 0.9

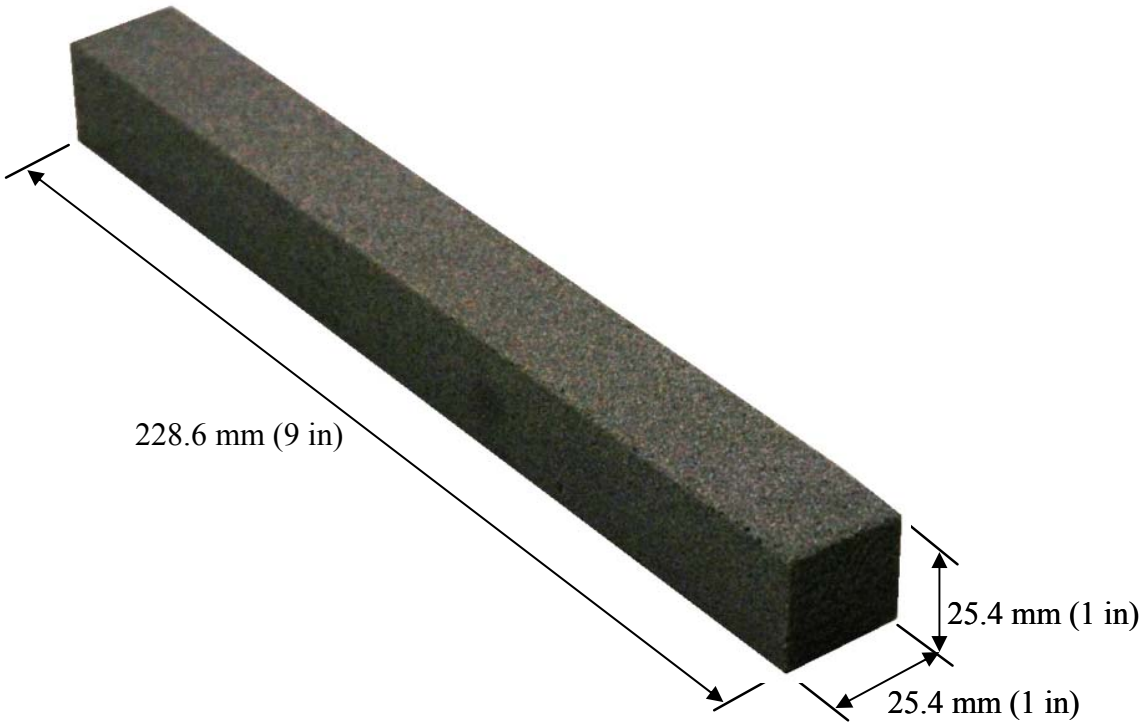

Figure 9: Photograph of a three-point bend specimen containing 1.25% binder by total weight at a 60:40 ratio of part 1 to part 2, and 3% black iron oxide by total weight.

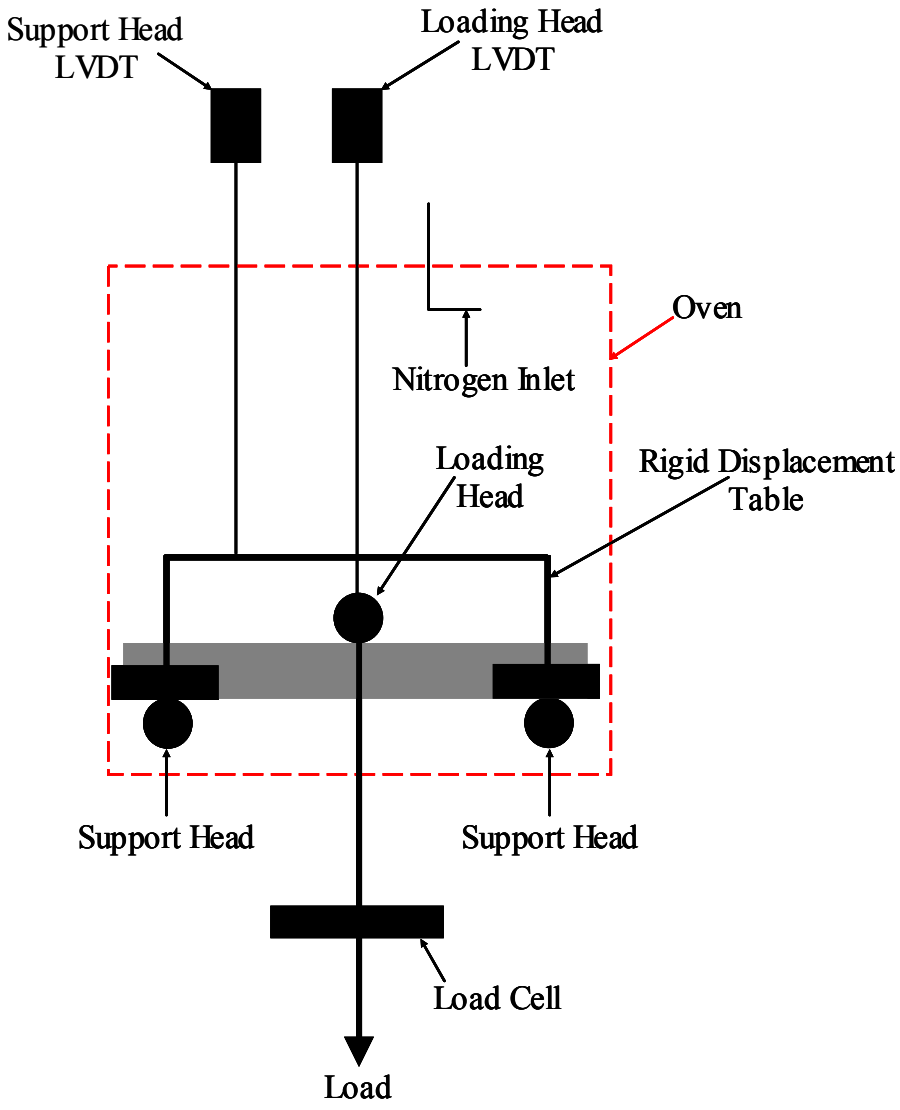

Figure 10: Schematic of three-point bend experimental setup.

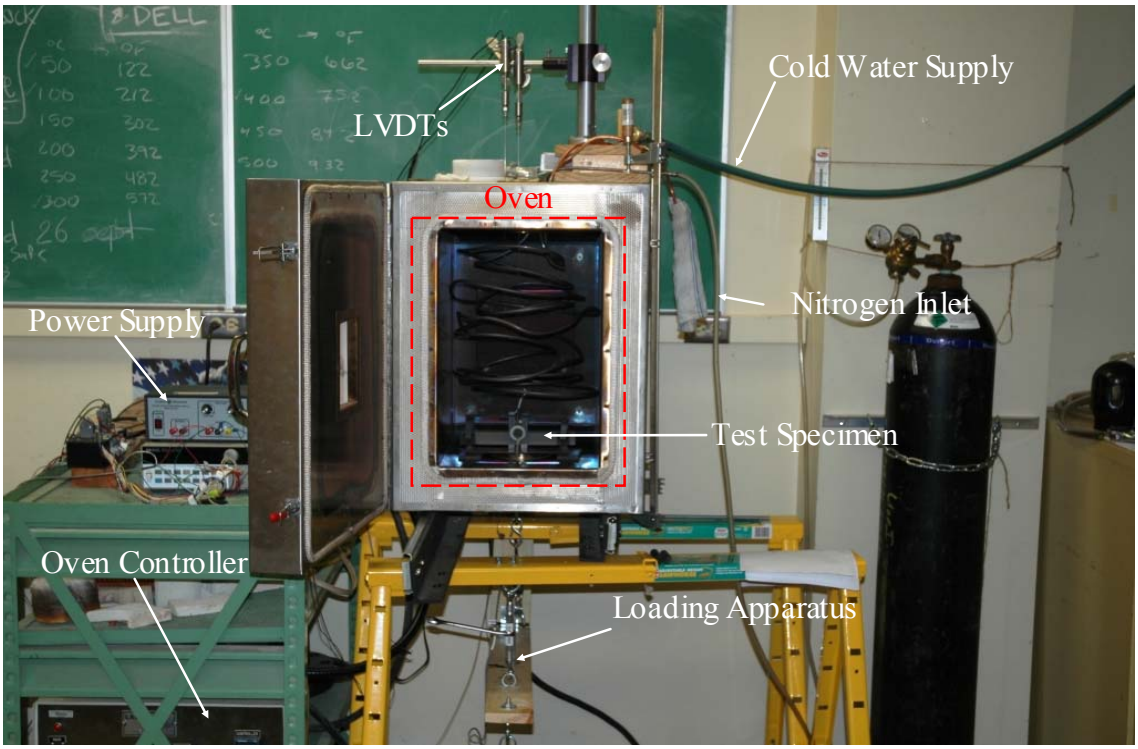

Figure 11: Photograph of the entire experimental setup.

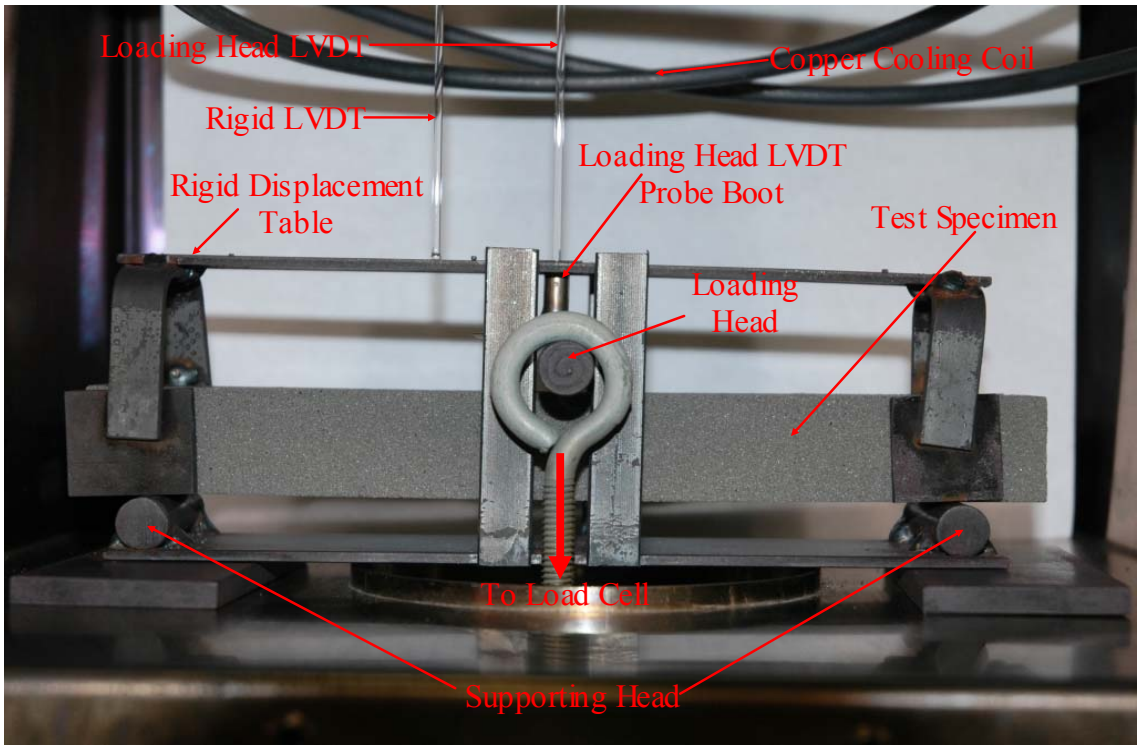

Figure 12: Photograph of the three-point bend fixture with a specimen inserted.

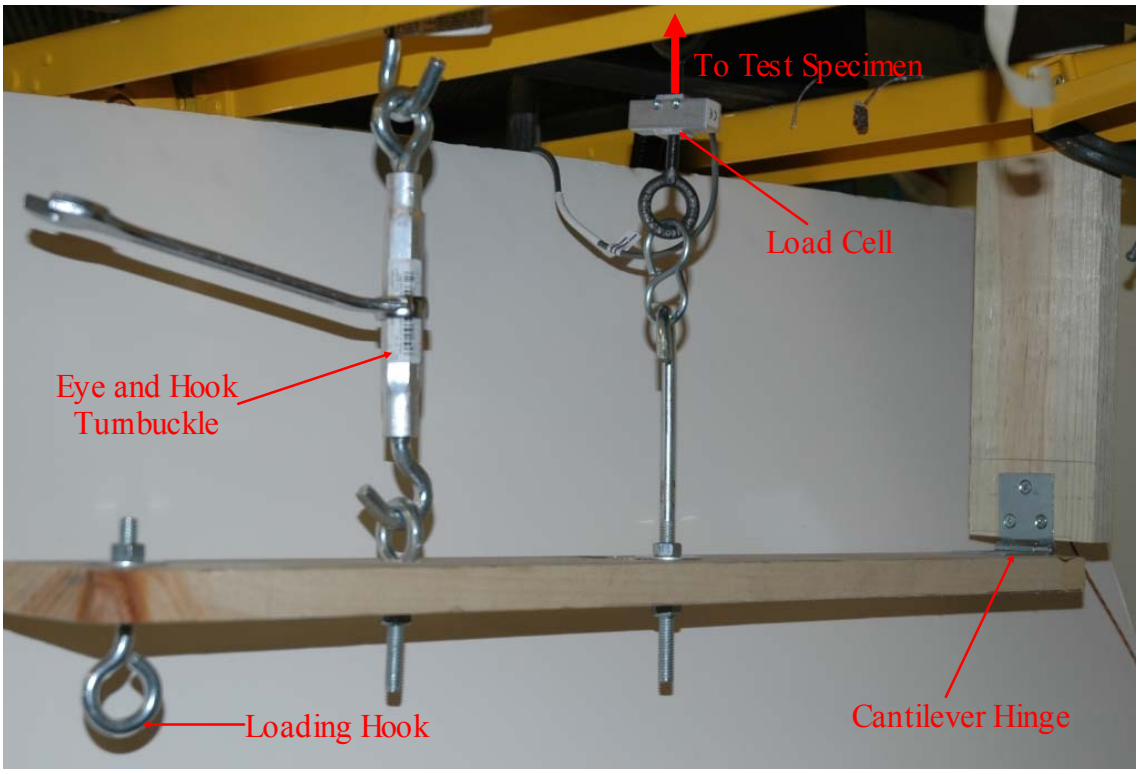

Figure 13: Photograph of the cantilever loading apparatus located underneath the oven.

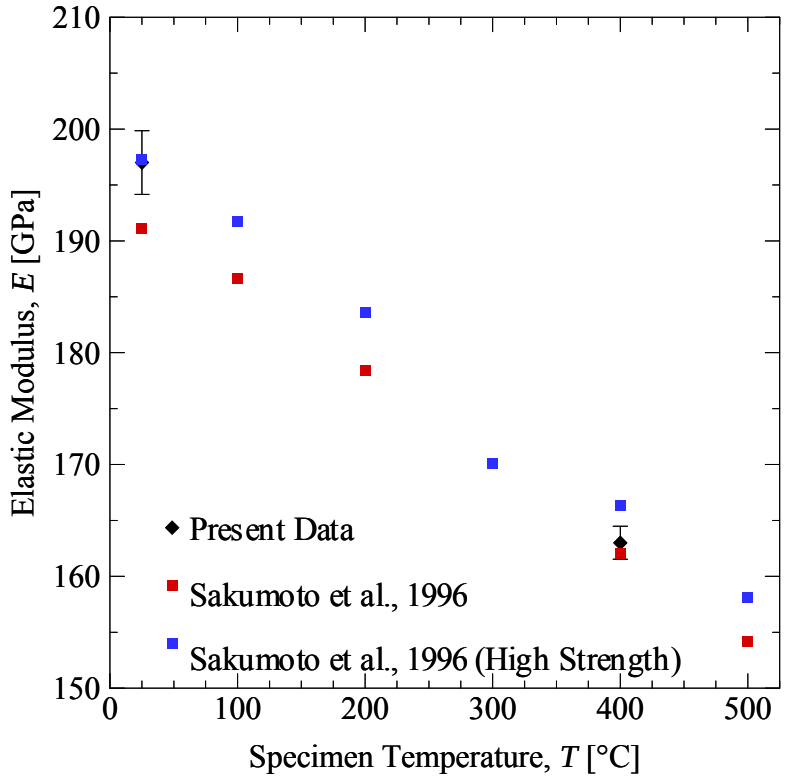

Figure 14: Comparison of present measurements of the elastic modulus of ASTM 304 stainless steel as a function of temperature with data from Sakumoto *et al.* [15].

Table 2: Sources of error in an elastic modulus measurement at room temperature.

Source of Error	Measured Value	± error
Span Length, *L* [mm]	190.56	± 0.01
Specimen Width, *b* [mm]	26.03	± 0.23
Specimen Thickness, *d* [mm]	25.50	± 0.02
Specimen Deflection, *D* [mm]	0.0766	± 0.0009
Applied Loading Force, *F* [N]	67.275	± 0.006

Table 3: Errors in the elastic modulus for a room temperature test.

	Elastic Modulus [MPa]		
Source of Error	R+	R-	±dR
Span Length, *L* [mm]	3521	3520	± 0.5
Specimen Width, *b* [mm]	3490	3552	± 31.0
Specimen Thickness, *d* [mm]	3512	3529	± 8.5
Specimen Deflection, *D* [mm]	3480	3562	± 41.0
Applied Loading Force, *F* [N]	3521	3520	± 0.5
Reported Elastic Modulus, *E* [MPa]	3520		± 52.1 ± (1.5%)

CHAPTER 4. RESULTS

4.1 Typical Stress-Strain Curves at Various Temperatures

Typical stress-strain curves from tests at four different specimen temperatures are presented in Figure 15. In these tests, the load was increased until the specimens broke. A straight line was fit to the elastic portion of the stress-strain curves, with the slope representing the measured elastic modulus. The same procedure for determining the elastic modulus was used for all tests, even though the specimens were usually not loaded until breaking. Figure 15 shows that at all temperatures the bonded sand behaves predominantly in an elastic manner, with failure occurring in a brittle mode. At the two intermediate temperatures, inelastic behavior is observed at high stresses. While the elastic behavior can be expected to be the same under any loading condition [5], the inelastic behavior is specific to the present three-point bend test. It can be seen from Figure 15 that the elastic modulus (i.e., the slope of the pink lines) varies strongly with temperature. This behavior is analyzed in more detail in the subsequent sub-sections. Tests in the next sections have repeated loading and unloading runs shown in Figure 16 unlike those from Figure 15 which were loaded once to breaking. Figure 16 shows a specimen heated at a constant rate while measuring the elastic modulus. Permanent deformation can be seen be the shift in the stress strain curves; this is due to a softening of the plastic binder and being loaded into the plastic regime. The ultimate strength and strain (at breaking) of the bonded sand also vary strongly with temperature. Detailed measurements of the ultimate strength of chemically bonded sand as a function of temperature can be found, for example, in References [7, 8]. The present study focuses solely on the elastic modulus.

4.2 Elastic Modulus Variation at an 8°C/min Heating Rate

Numerous tests were performed for an average heating rate of 8°C/min. As indicated in Figure 7 by a dashed line, this heating rate is typical for locations in the mold

that are between 1 in and 3 in away from the mold-metal interface. Figure 17 shows the elastic modulus measurements as a function of time for a typical test. The elastic modulus measurements in Figure 17 were measured from the stress-strain data shown in Figure 16. Superimposed on Figure 17 are the measured specimen temperatures at the center and surface. It can be seen that the center and surface temperatures are always within 10°C of each other. The specimen was heated to about 500°C; at this temperature the strength of the specimen approached zero and no elastic modulus measurements could be performed at higher temperatures. As can be seen from the slope of the temperature curves, the heating rate is not completely constant, but varies by less than ±3°C/min during the test. There are approximately 80 elastic modulus measurements plotted in Figure 17, implying that approximately one measurement was performed per minute. This results in an almost continuous variation of the elastic modulus with temperature.

Figure 18 shows elastic modulus measurements for seven different specimens that were all heated at a rate of 8.1±1.4°C/min. Here, the elastic modulus is plotted directly against the measured temperature. Three of specimens contained black iron oxide and four did not. It can be seen that there is no discernable difference in the elastic modulus between the two types of specimens. This indicates that the addition of black iron oxide has no effect on the elastic modulus. All data fall within a relatively narrow band and were fit to a line by equally weighting all seven specimens shown in Figure 18. In addition, Figure 18 shows the average of all room temperature elastic modulus measurements for the seven specimens. This average is equal to 3,613 MPa, with a standard deviation of 569 MPa. The fit line levels out to a room temperature elastic modulus lower than the average due to bias errors between specimens as can be seen in Figure 18, where specimens have non-uniform runs.

The variation of the elastic modulus with temperature can be best described by following the black line in Figure 18. The elastic modulus decreases steeply around 60°C with increasing temperature from the room temperature value of 3,613 MPa to about 600

MPa at 125°C. Between 125°C and 250°C, the elastic modulus is relatively constant. Above 250°C, it increases to 1,200 MPa at 280°C and then decreases again to 800 MPa at 350°C. Above 350°C, the elastic modulus increases almost linearly with temperature until it reaches 2,200 MPa at 500°C.

These above variations correlate well with the chemical reactions the binder undergoes during heating. Giese *et al*. [16] measured the energy released during heating (at a 10°C/min rate) of a 60:40 PUNB sample using differential scanning calorimetry (DSC). The various peaks in the DSC curve were associated with specific changes in the binder composition. Figure 19 shows the findings of Giese *et al*. [16] superimposed on the fit of the elastic modulus data from Figure 18. It can be seen that the start of solvent vaporization corresponds to a small kink in the elastic modulus curve at about 65°C. The end of solvent vaporization coincides with the elastic modulus reaching the 600 MPa value at about 125°C. The start of urethane bond breakage at 180°C can also be associated with a small kink in the elastic modulus curve. The peak in the elastic modulus around 280°C coincides with the maximum decomposition rate and the end of urethane bond breakage. Most importantly, the linear increase in the elastic modulus above 350°C can be associated with the breakdown of the binder to polymer aromatics.

4.3 Effect of Solvent

The results shown in Figure 19 indicate that the solvent in the binder may have an effect on the elastic modulus. Therefore, additional tests were performed where the solvent was removed from the specimens prior to testing by heating them to 140°C and allowing them to cool down to room temperature again. Giese *et al*. [16] report from DSC results that this method removes the solvents from the system without affecting higher temperature reactions. The results of three such tests (at a 8°C/min heating rate) are shown in Figure 20 and compared to the fit of the elastic modulus data from Figure 18 (without solvent removal). Despite the scatter in the data, it can be seen that the

solvent has an effect on the elastic modulus at temperatures below about 150°C. While the room temperature elastic modulus is approximately the same with and without solvent, the elastic modulus between 50°C and 150°C is generally higher with than without solvent removal. The differences can be as large as a factor of two. However, at temperatures above 150°C, Figure 20 shows that the elastic modulus of the specimens with the solvent removed follows the same variation with temperature as the fit of the elastic modulus data from the seven original specimens where the solvent was not removed.

4.4 Elastic Modulus Variation at Various Heating Rates

In order to investigate the effect of heating rate, additional tests were performed at lower heating rates of 0.8, 2, and 5°C/min. Lower heating rates were chosen over higher heating rates which are more common in castings due to limitations of the oven. In view of Figure 7, such a low heating rates occur in a steel casting molds far from the mold-metal interface (greater than 3 in). The results for the elastic modulus variation with temperature for all continuous heating rates are shown in Figure 21 and compared to the fit of the elastic modulus data from Figure 18 for a heating rate of 8°C/min. It can be seen that the elastic modulus follows the same variation for all heating rates at temperatures below about 125°C. At higher temperatures, however, the lower heating rates show consistently higher elastic moduli than the 8°C/min data. The general trends in the variation with temperature are similar for the heating rates; the elastic modulus starts to increase at lower temperatures rather than staying constant as for the 8°C/min heating rate. At about 250°C, the elastic modulus for the 2°C/min heating rate is equal to 1,400 MPa, while it is still at 600 MPa for the 8°C/min heating rate. At 400°C, the elastic moduli are approximately 2,800 MPa and 1,400 MPa for the 2°C/min and 8°C/min heating rates, respectively. The elastic modulus of the slower heating rates peak at approximately 2,800 MPa with the 0.8°C/min heating rate peaking first and 5°C/min

heating rate peaking last. The elastic modulus for the three slower heating rates show a significant decrease before the specimen breaks at approximately 475°C. The fact that the heating rate has such a strong effect on the elastic modulus indicates that the chemical changes of the binder during heating, in particular the urethane bond breakage, are very time dependent.

4.5 Elastic Modulus during Holding at Elevated Temperatures

The strong dependence of the elastic modulus on the heating rate observed in Figure 21 raises the question what the elastic modulus variation is for an infinitely slow heating rate. Does the elastic modulus at a given temperature above 150°C continue to increase with decreasing heating rate? In order to investigate this issue, a special set of experiments was conducted where a specimen was heated (at approximately 8°C/min) to a pre-selected "hold" temperature and then held at this temperature for a time sufficient for the elastic modulus to attain a constant "steady-state" value. Results are shown in Figure 22 to Figure 39 for eighteen different holding temperatures from 50°C to 440°C. In each of the graphs, the measured elastic modulus and temperature are plotted as a function of time. It can be seen that during the heating period, the elastic modulus varies in a similar fashion as already discussed in connection with Figure 17. However, during holding of the specimen at a given temperature, the elastic modulus can be seen to continue to change with time, except for the experiment with the lowest holding temperature (50°C, Figure 22). For the higher hold temperatures, the elastic modulus always increases during the holding period, until the constant steady-state value is achieved or hits a maximum followed by binder degradation.

The constant steady-state values for the elastic modulus measured in the present set of experiments are plotted as a function of the hold temperature in Figure 40. It can be seen that the steady-state value for the elastic modulus for a hold temperature of 50°C is

close to the instantaneous value measured in the continuous heating experiments. This is expected since the boiling point of the solvents start at approximately 65°C as reported by Giese *et al*. [16]. For hold temperatures between 100°C and 200°C, the steady-state elastic modulus is equal to about 2,000 MPa. The steady-state elastic modulus suddenly increases around 200°C from 2,000 MPa to 3,200 MPa at 280°C followed by a sharp drop at 300°C to 2,400 MPa. The steady-state elastic modulus remains constant after 300°C until 350°C, the elastic modulus then starts to decrease until 410°C at which point a steady-state elastic modulus is never reached due to the continual degradation of the binder. These steady-state values are much higher than the instantaneous values measured during the continuous heating experiments for temperatures below 325°C as shown in Figure 41. Above 325°C, the steady-state value approaches the instantaneous value measured for the slower heating rates. The sudden decrease in the steady-state elastic modulus above 375°C agrees with the slower heating rate peaks during which the binder starts to rapidly deteriorate.

The steady-state elastic modulus as a percentage of the specimens' room temperature elastic modulus as plotted against the holding temperature in Figure 41. A linear decrease in the room temperature percentage from 100% at room temperature to approximately 57% at 125°C can be seen. The percentage remains constant from 125°C to 200°C, at which point an increase from 57% to 70% is observed with a spike of 80% at 250°C. Between 380°C and 410°C a sudden decrease is observed due to continuous binder degradation as reported by Giese *et al*. [16] when the binder starts to break down to polymer aromatics.

It should also be noted that the steady-state elastic moduli measured in the present set of experiments are in close agreement with those measured in References [7, 8]. This can be expected because the specimens in the experiments of References [7, 8] were held at elevated temperatures for some time before the elastic modulus measurement was performed.

4.6 Retained Room Temperature Elastic Modulus After Holding at an Elevated Temperature

After the specimens of Section 4.5 were held at an elevated temperature for a long period of time, the power to the oven was shut off and the cooling system was activated. The oven was allowed to cool until the specimens were back at room temperature. Then, measurements of the retained room temperature elastic modulus were performed for each specimen. The results of these measurements are shown in Figure 22 to Figure 39 and also plotted as a function of the elevated hold temperature prior to cooling in Figure 43. Figure 43 shows that for a hold temperature of 50°C to 78°C the specimens fully recover their initial room temperature stiffness.

However, for hold temperatures above 100°C, the retained elastic modulus at room temperature is consistently lower than the initial room temperature value before any heating. This reduction in the room temperature elastic modulus indicates permanent degradation of the binder when heated to temperatures above the boiling point of the solvent. Such a permanent degradation can be expected since the binder undergoes irreversible chemical reactions during heating. For hold temperature between 125°C and 300°C, the urethane bonds break (Figure 19), and the retained room temperature elastic modulus is between 2,900 MPa and 3,400 MPa. These values should be compared to an average initial room temperature elastic modulus of 3,600 MPa. They are, however, higher than the steady state elastic moduli measured at the hold temperature (~2000 MPa, Figure 40), indicating that the specimens regain some stiffness upon cooling.

For hold temperatures above 340°C in Figure 43, a much stronger degradation of the room temperature elastic modulus can be observed. At this hold temperature, the retained room temperature elastic modulus is equal to about 1,200 MPa, compared to 3,600 MPa before heating. This stronger degradation can be expected because at about 350°C the binder starts to break down to polymer aromatics (Figure 19). A comparison of Figures 43 and 44 shows that even for the 370°C and 380°C hold temperatures the

bonded sand retains most of its stiffness upon cooling to room temperature. Above 380°C, the binder degrades so rapidly that the specimen breaks even under low loads making high temperature retained elastic modulus tests impossible.

As for the steady-state elastic modulus, the retained room temperature elastic modulus values are also plotted as a percentage of the specimens' initial room temperature elastic modulus in Figure 44. The full recovery upon cooling can be seen much better for holding temperatures less than 100°C. For all specimens held at or above 100°C, an observable decrease can be seen with two relatively constant values of 75% and 85% for temperatures between 100°C to 200°C and 200°C to 250°C. This agrees with the DSC study of Giese *et al*. in Figure 19 where the transition points match with the temperatures associated with specific reactions. Likewise, the initial slow decrease in the retained elastic modulus from the initial room temperature elastic modulus starting at 250°C followed by a much more rapid decrease in percentage retained starting at 350°C can be attributed to the breakdown of PU bonds and breakdown of Polymer Aromatics respectfully.

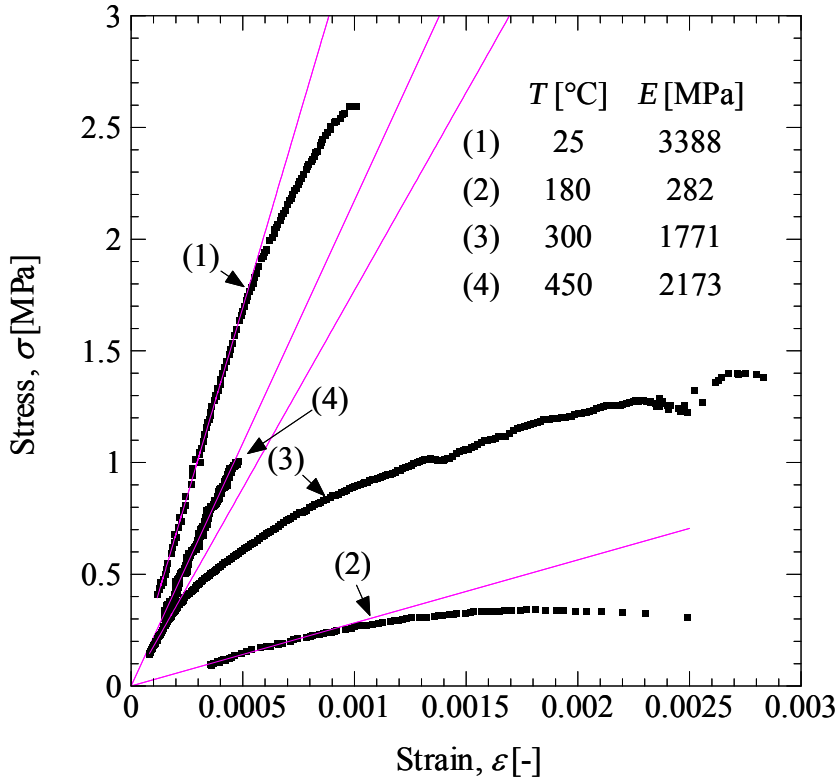

Figure 15: Typical stress-strain curves at four different temperatures loaded until breaking with a linear best fit line for the data in the elastic regime.

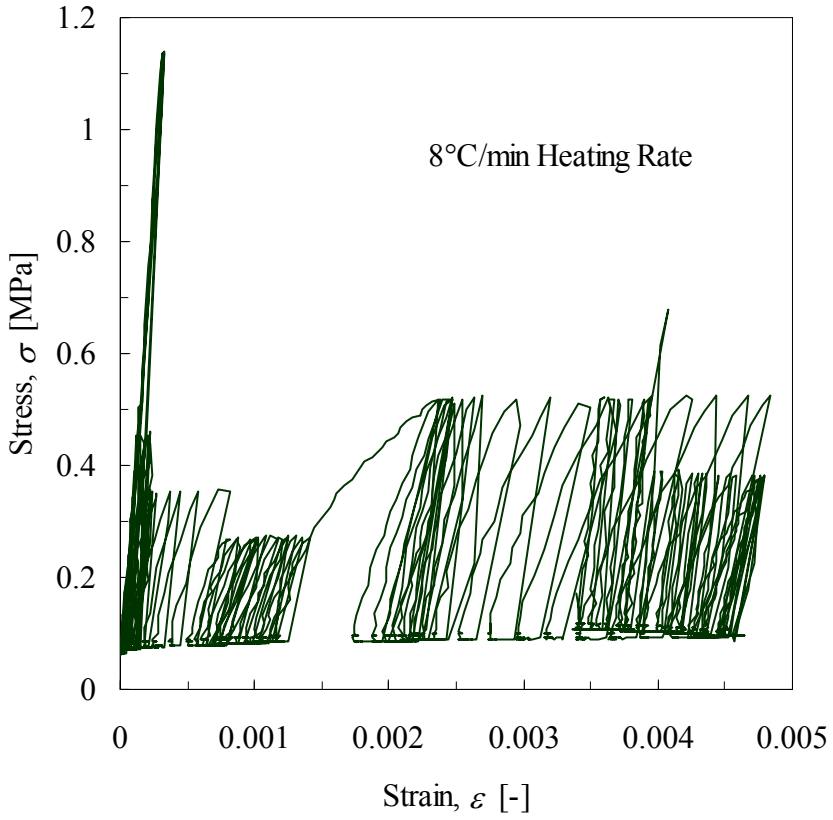

Figure 16: Stress-Strain curve for a single specimen under constant heating at 8°C/min with repeated loading and unloading until the strength of the specimen approaches zero.

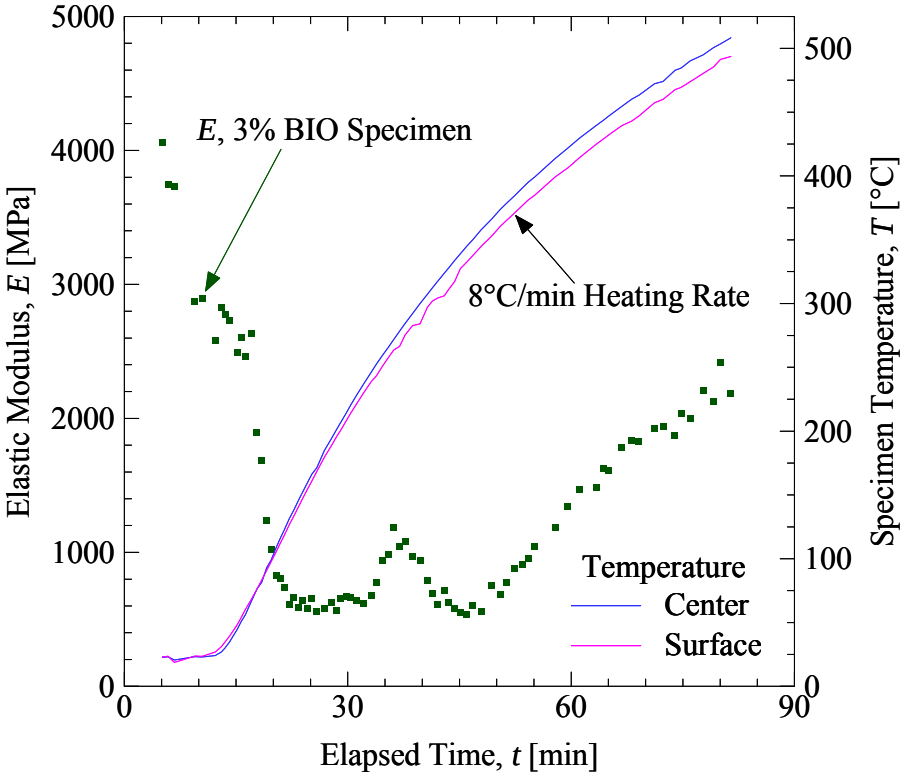

Figure 17: Measured elastic modulus and temperatures as a function of time for a typical test with an average heating rate of 8°C/min from stress-strain data in Figure 16.

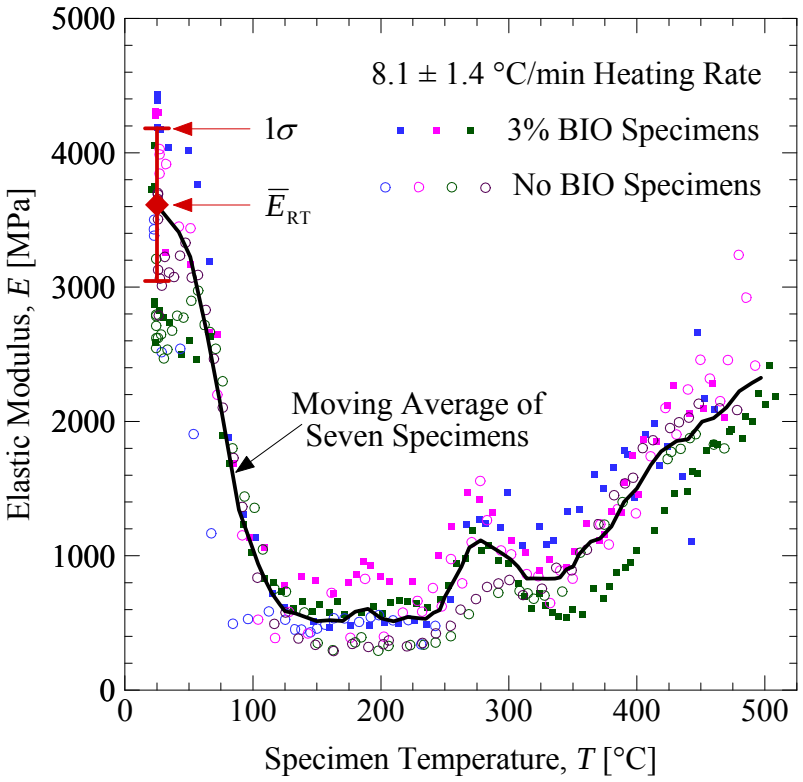

Figure 18: Measured elastic modulus as a function of temperature for an average heating rate of 8°C/min.

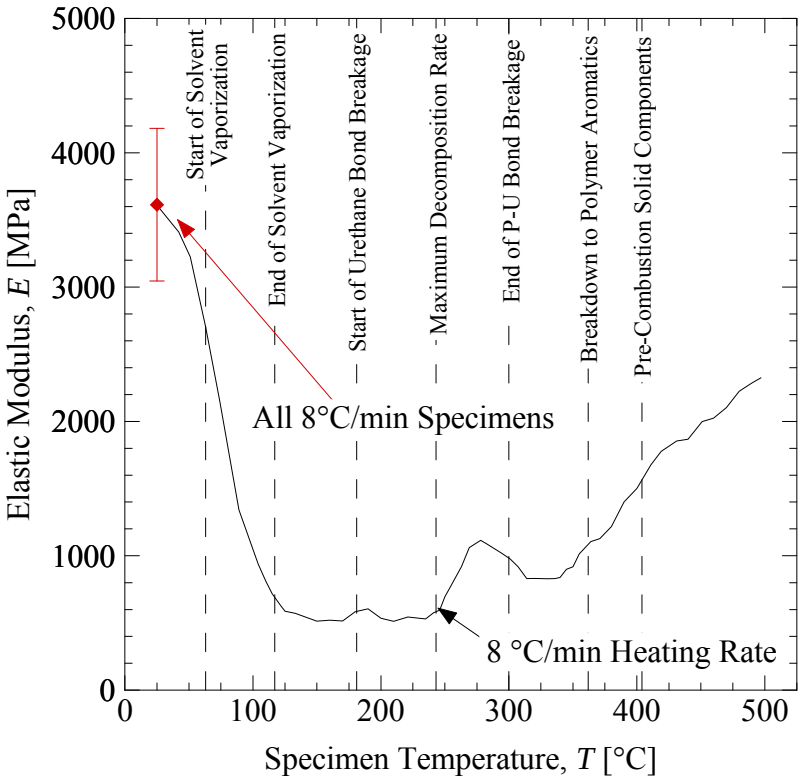

Figure 19: Comparison of the measured elastic modulus variation with the DSC data from Giese *et al*. [16] for a 60:40 ratio PUNB sample heated at 10°C/min.

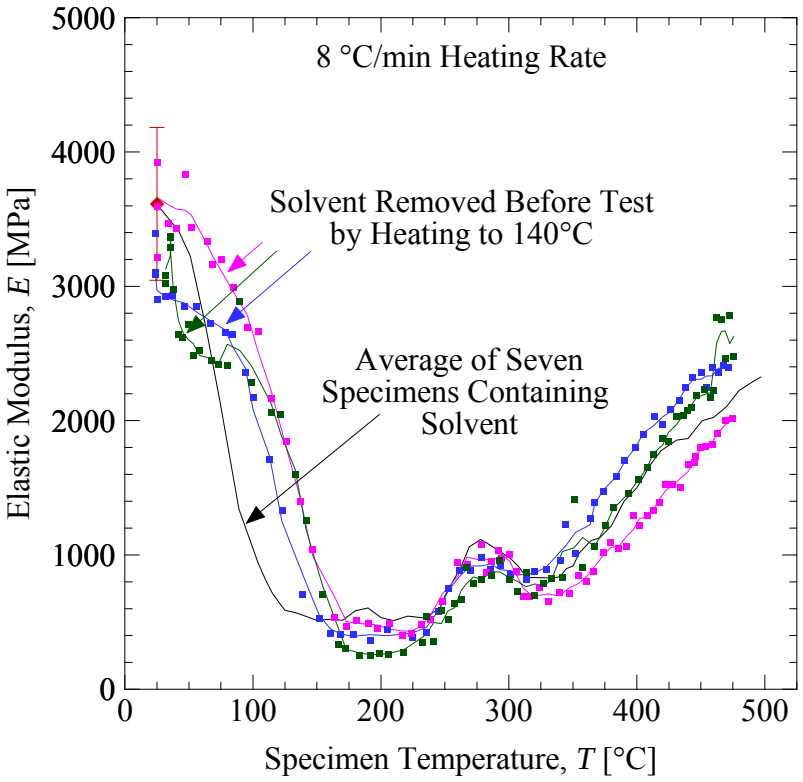

Figure 20: Comparison of the elastic modulus variation with temperature for specimens with and without solvent.

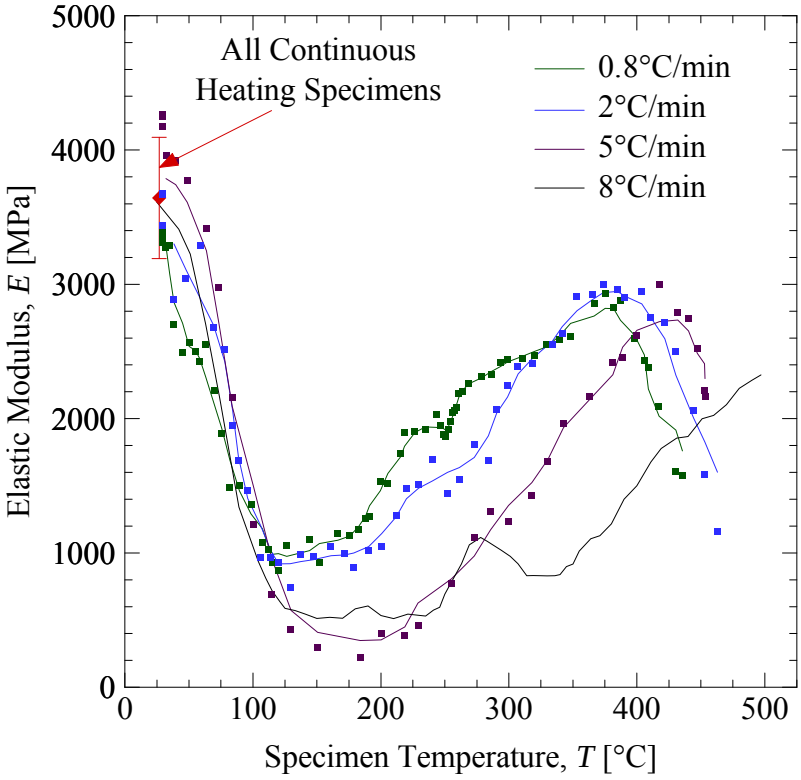

Figure 21: Comparison of the elastic modulus variation with temperature for specimens heated at 0.8, 2, 5, and 8°C/min.

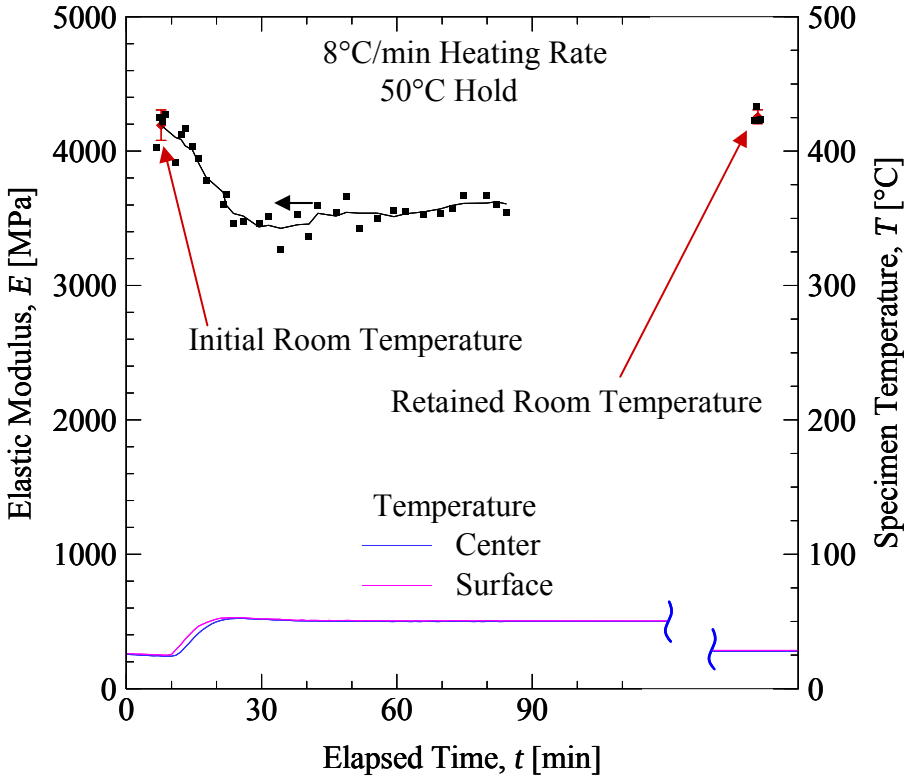

Figure 22: Elastic modulus variation during heating and holding at 50°C until a steady-state value is attained and retained elastic modulus after cooling to room temperature.

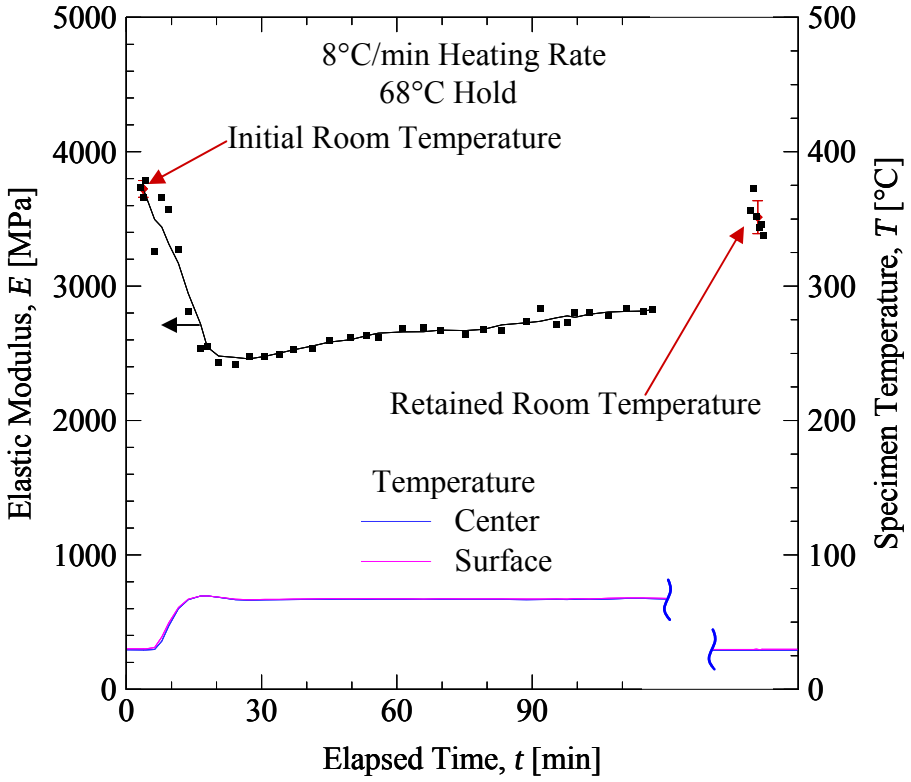

Figure 23: Elastic modulus variation during heating and holding at 68°C until a steady-state value is attained and retained elastic modulus after cooling to room temperature.

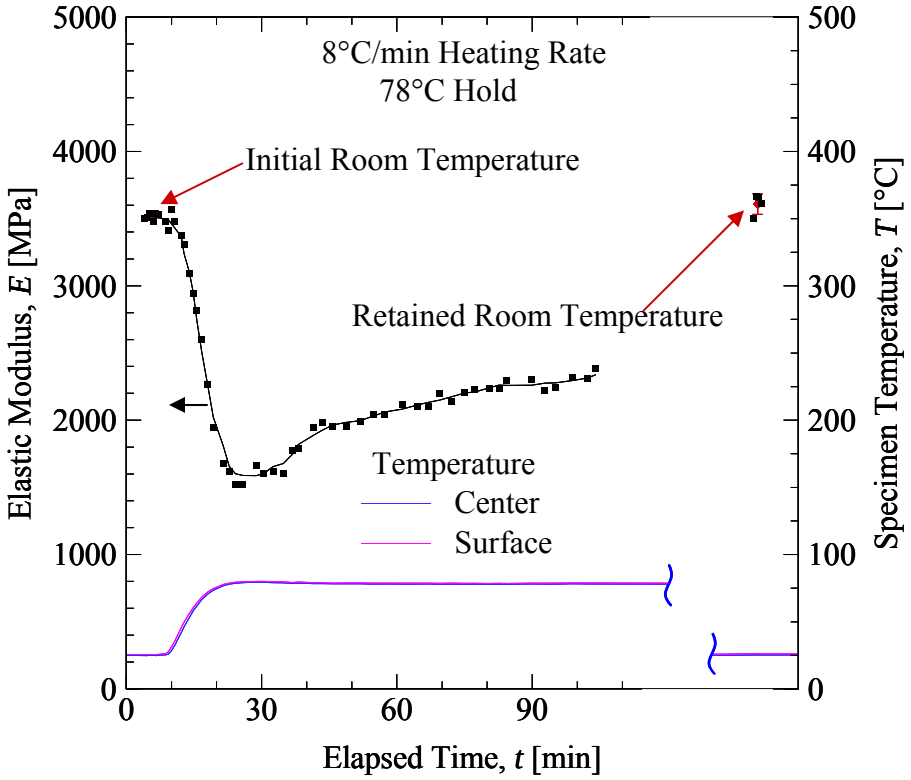

Figure 24: Elastic modulus variation during heating and holding at 78°C until a steady-state value is attained and retained elastic modulus after cooling to room temperature.

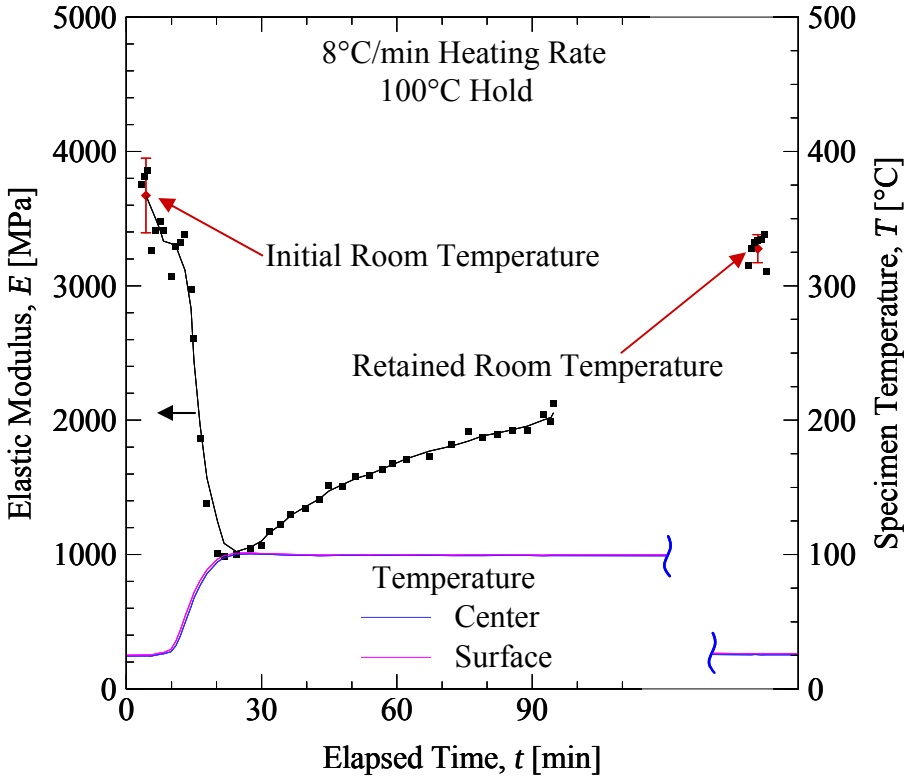

Figure 25: Elastic modulus variation during heating and holding at 100°C until a steady-state value is attained and retained elastic modulus after cooling to room temperature.

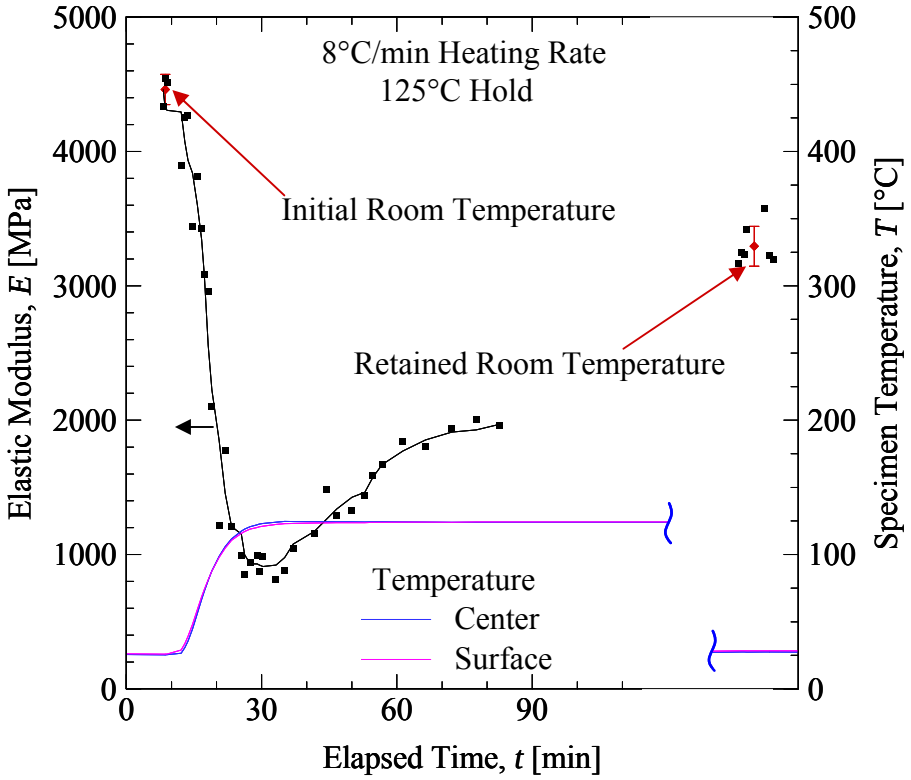

Figure 26: Elastic modulus variation during heating and holding at 125°C until a steady-state value is attained and retained elastic modulus after cooling to room temperature.

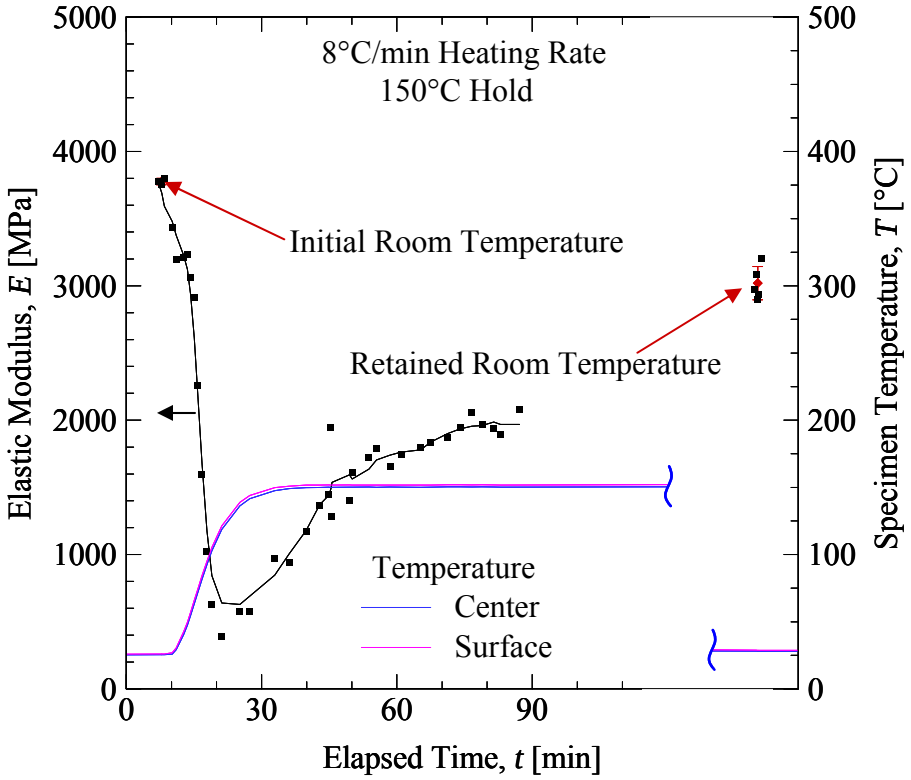

Figure 27: Elastic modulus variation during heating and holding at 150°C until a steady-state value is attained and retained elastic modulus after cooling to room temperature.

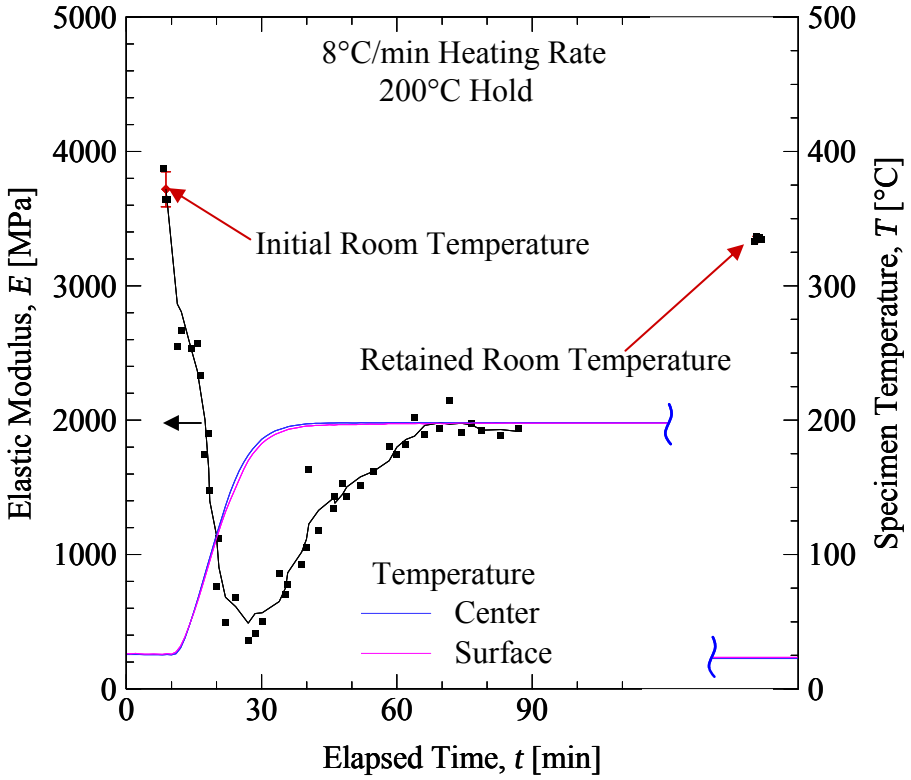

Figure 28: Elastic modulus variation during heating and holding at 200°C until a steady-state value is attained and retained elastic modulus after cooling to room temperature.

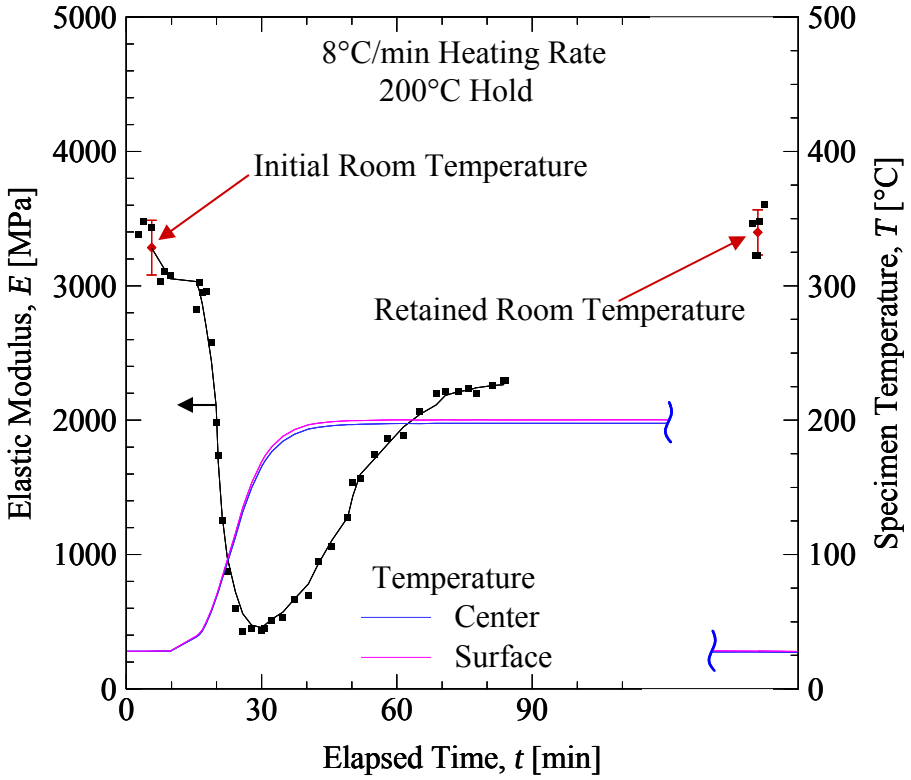

Figure 29: Elastic modulus variation during heating and holding at 200°C until a steady-state value is attained and retained elastic modulus after cooling to room temperature.

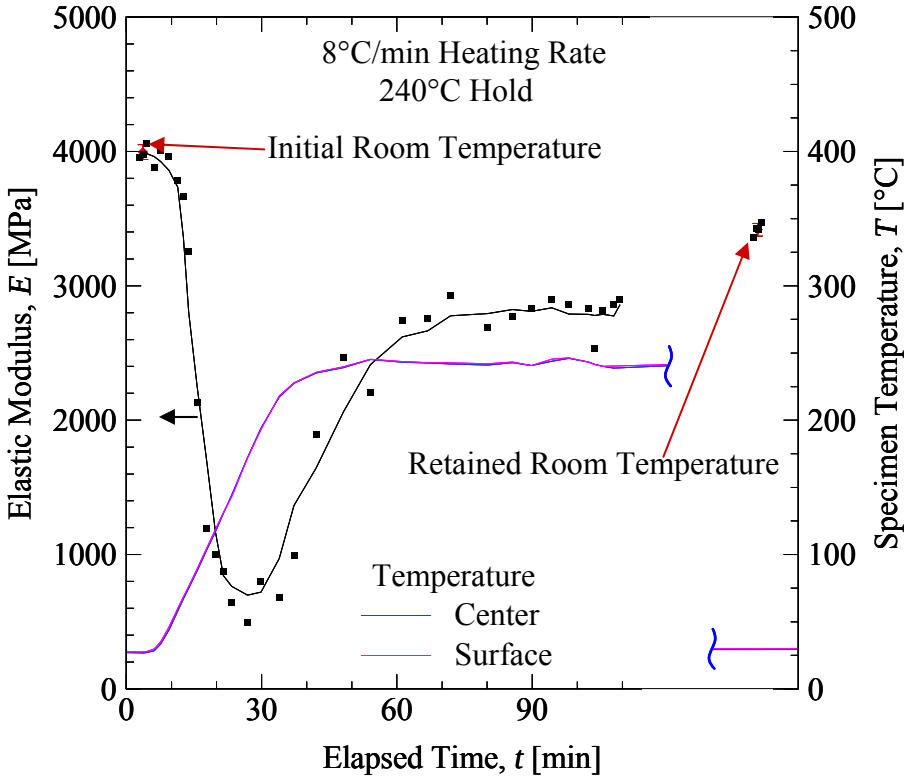

Figure 30: Elastic modulus variation during heating and holding at 240°C until a steady-state value is attained and retained elastic modulus after cooling to room temperature.

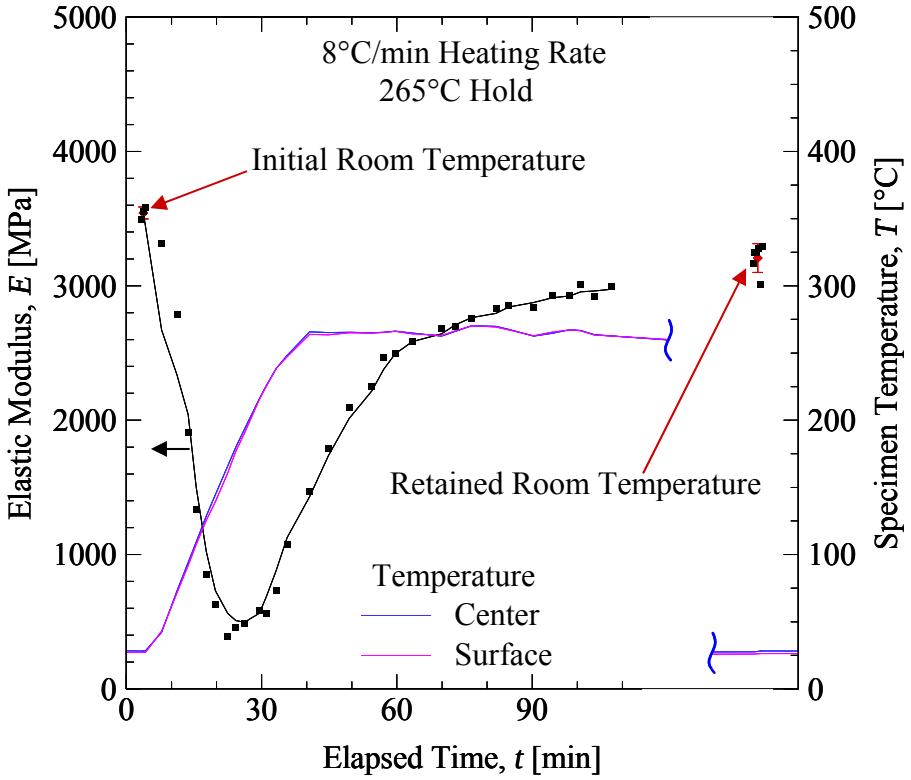

Figure 31: Elastic modulus variation during heating and holding at 265°C until a steady-state value is attained and retained elastic modulus after cooling to room temperature.

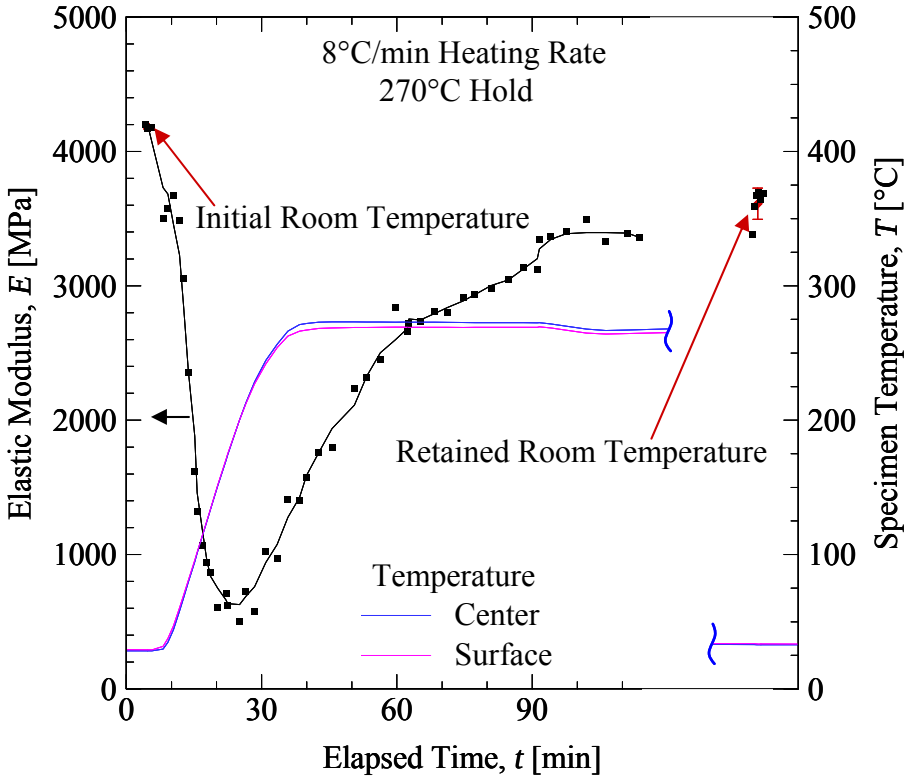

Figure 32: Elastic modulus variation during heating and holding at 270°C until a steady-state value is attained and retained elastic modulus after cooling to room temperature.

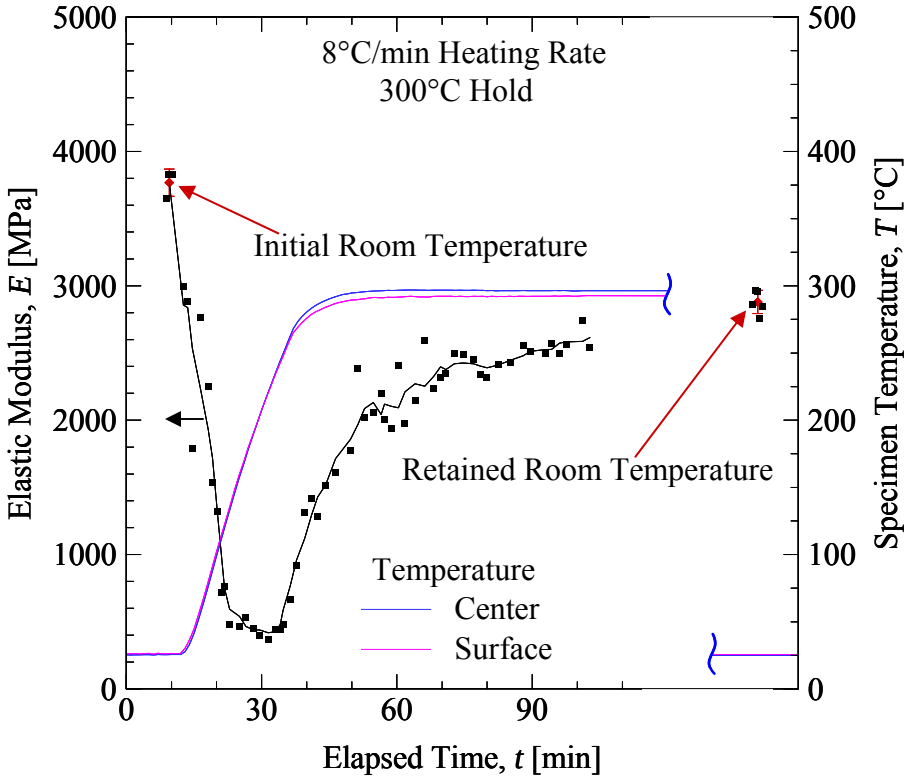

Figure 33: Elastic modulus variation during heating and holding at 300°C until a steady-state value is attained and retained elastic modulus after cooling to room temperature.

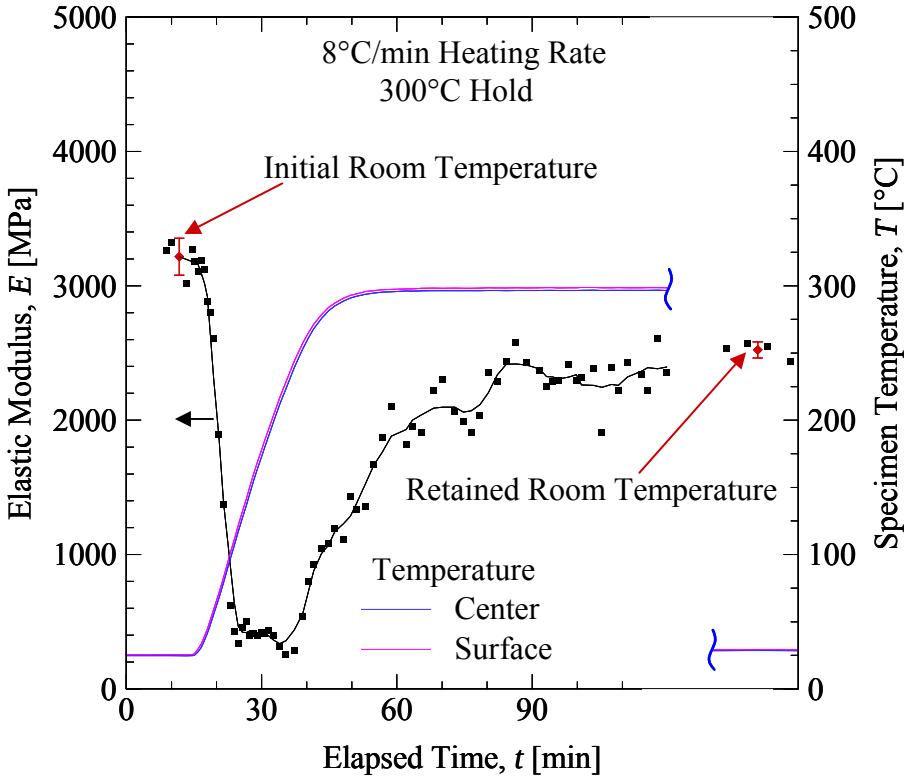

Figure 34: Elastic modulus variation during heating and holding at 300°C until a steady-state value is attained and retained elastic modulus after cooling to room temperature.

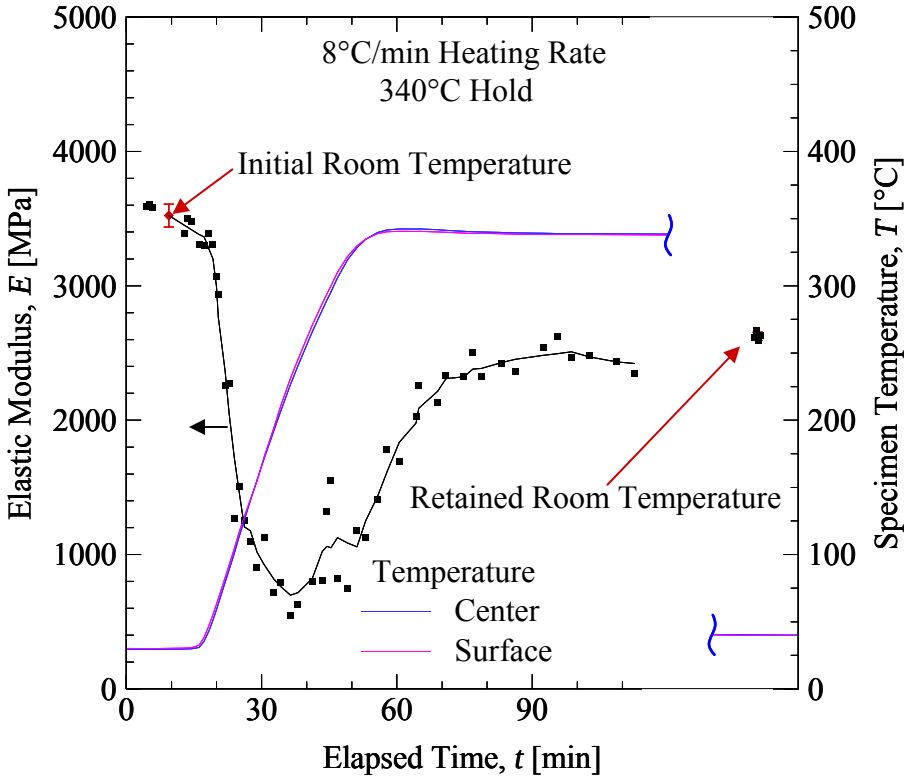

Figure 35: Elastic modulus variation during heating and holding at 340°C until a steady-state value is attained and retained elastic modulus after cooling to room temperature.

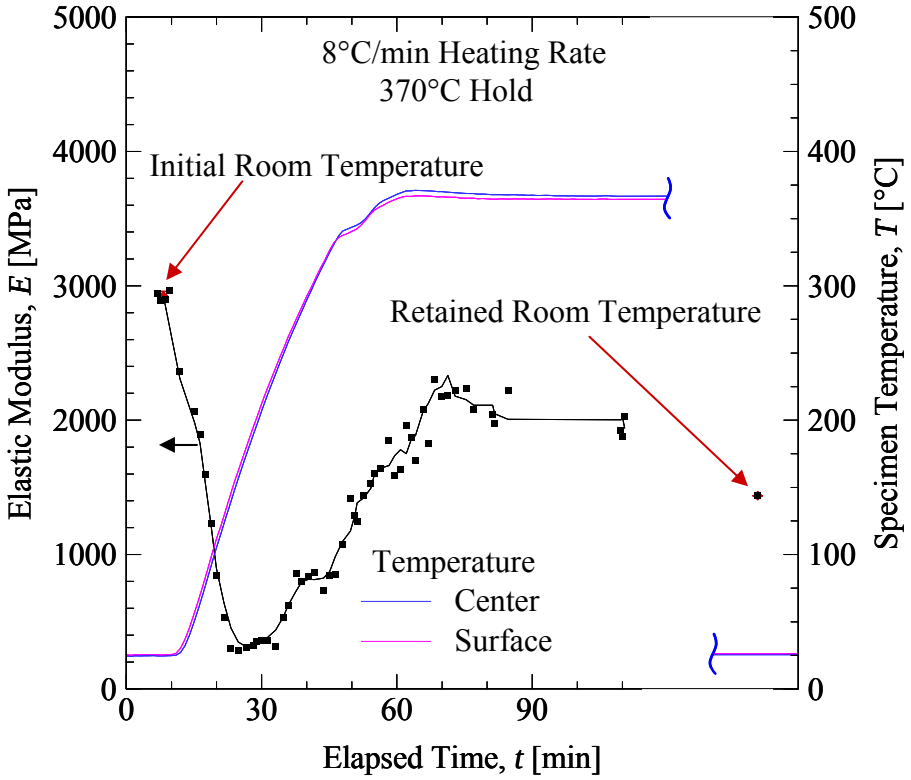

Figure 36: Elastic modulus variation during heating and holding at 370°C until a steady-state value is attained and retained elastic modulus after cooling to room temperature.

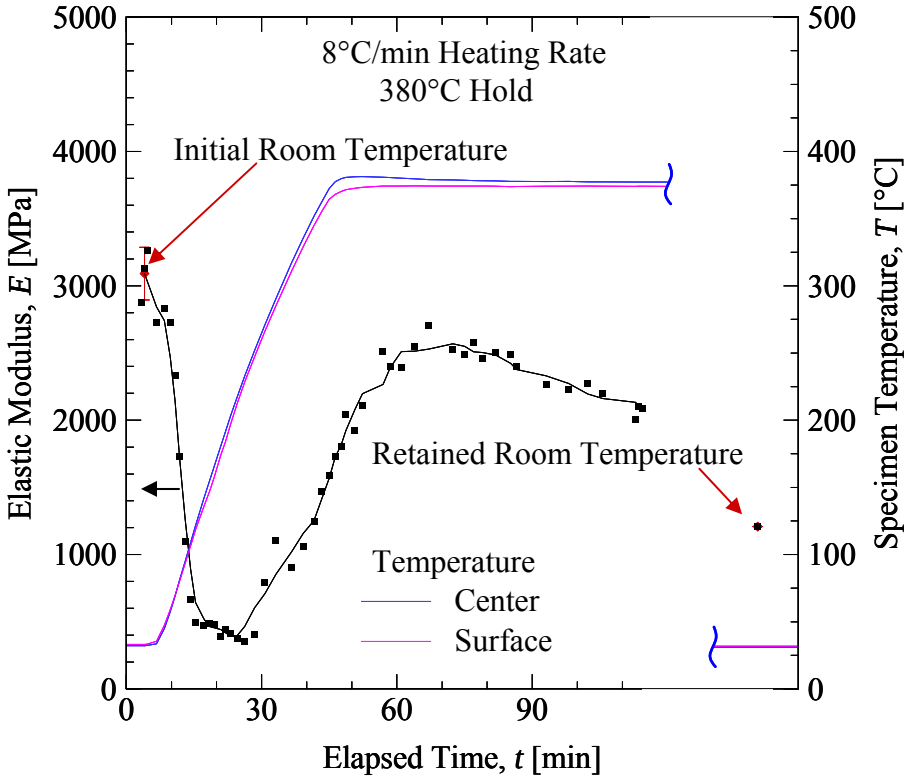

Figure 37: Elastic modulus variation during heating and holding at 380°C until a steady-state value is attained and retained elastic modulus after cooling to room temperature.

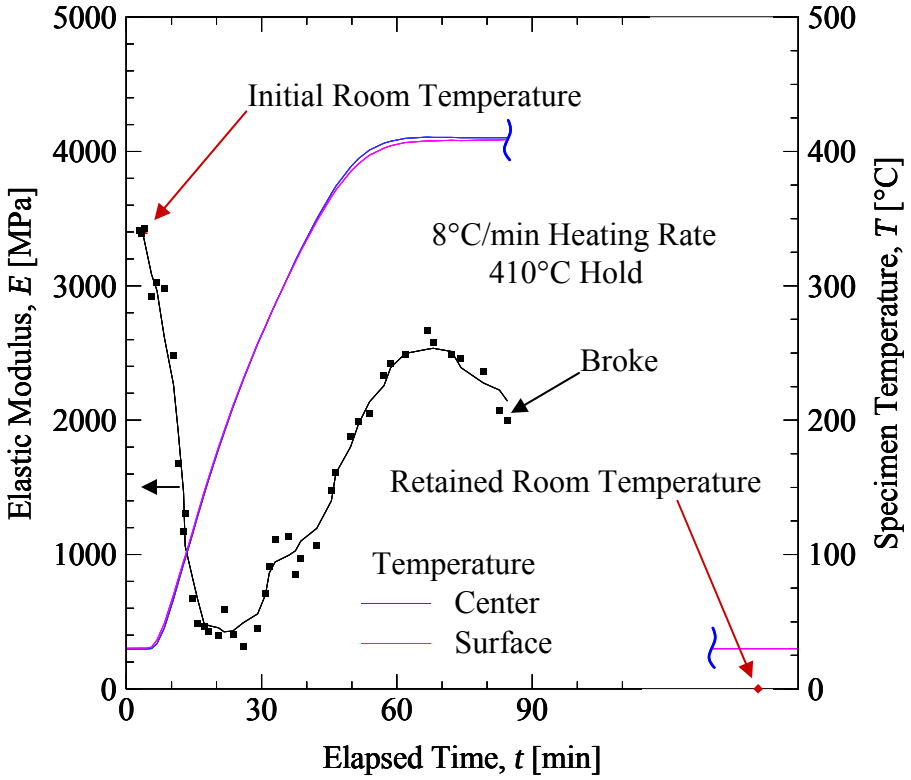

Figure 38: Elastic modulus variation during heating and holding at 410°C until a steady-state value is attained and retained elastic modulus after cooling to room temperature.

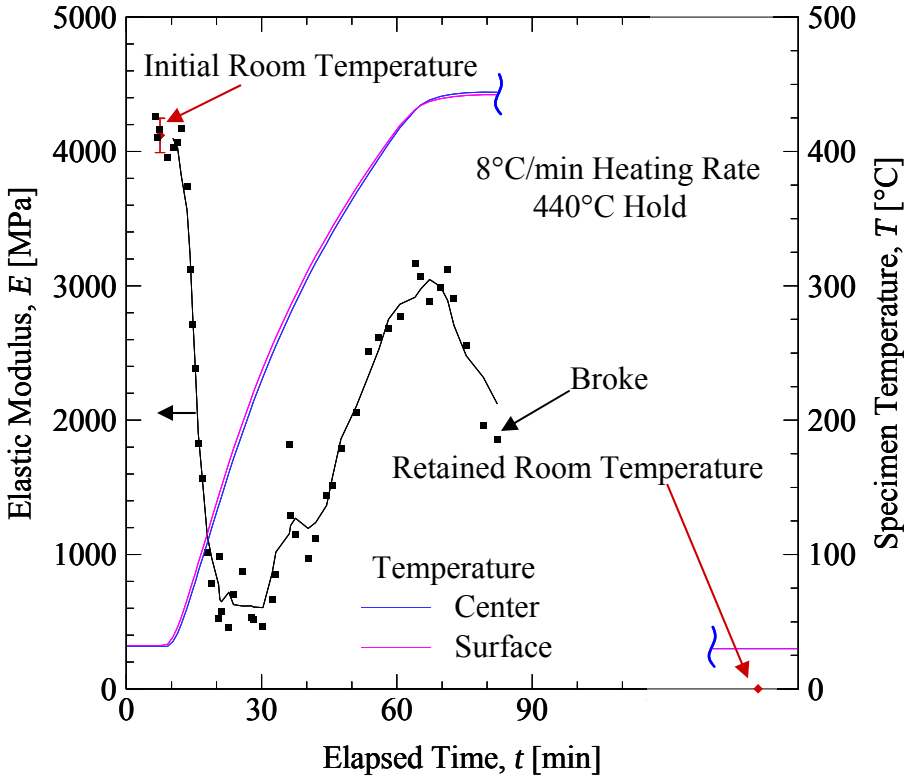

Figure 39: Elastic modulus variation during heating and holding at 440°C until a steady-state value is attained and retained elastic modulus after cooling to room temperature.

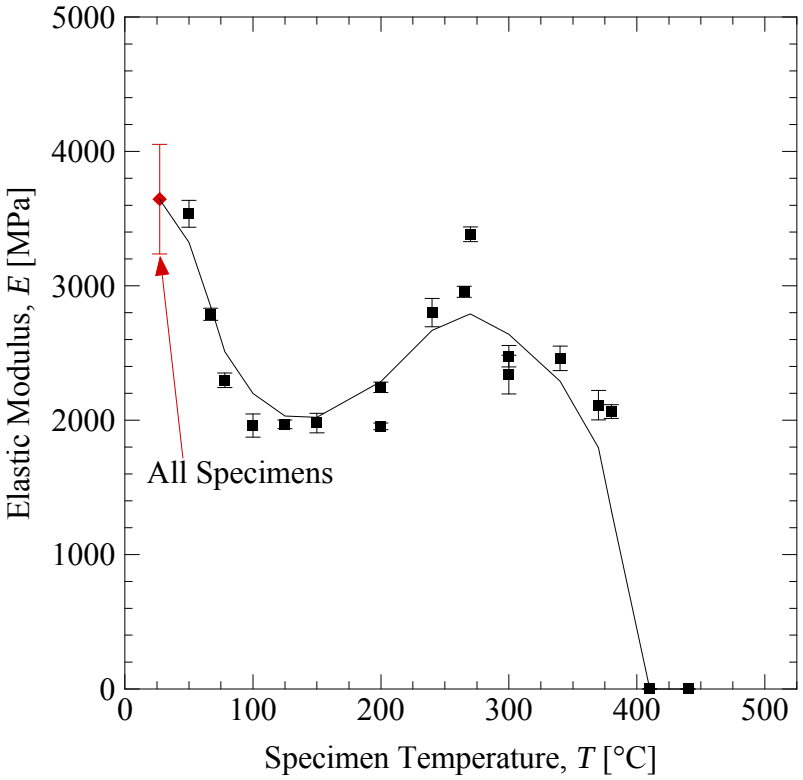

Figure 40: Steady-state system elastic modulus as a function of the hold temperature with a moving average trend line.

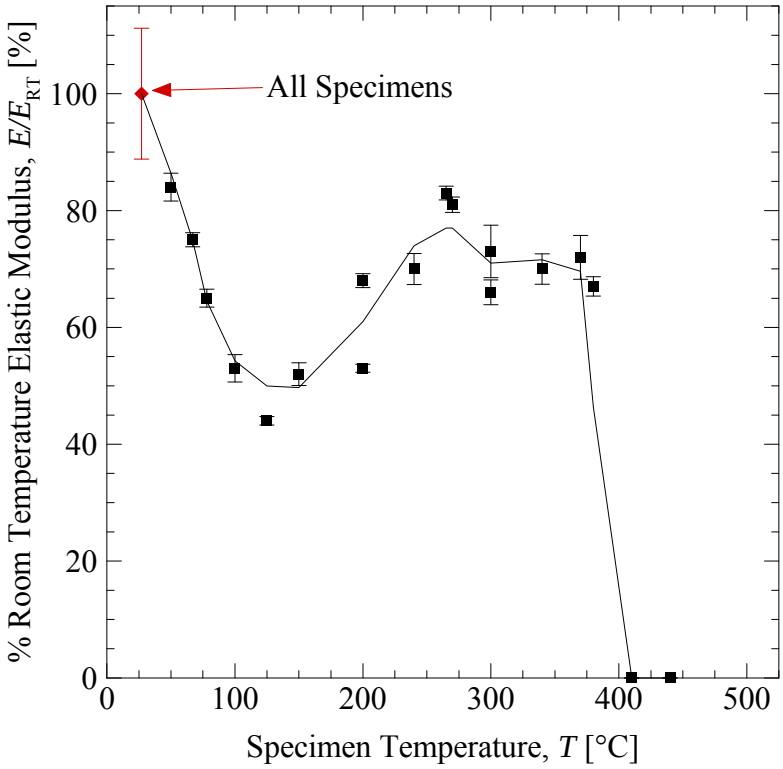

Figure 41: Steady-state system elastic modulus percent of specimens' initial room temperature elastic modulus as a function of the hold temperature with a moving average trend line.

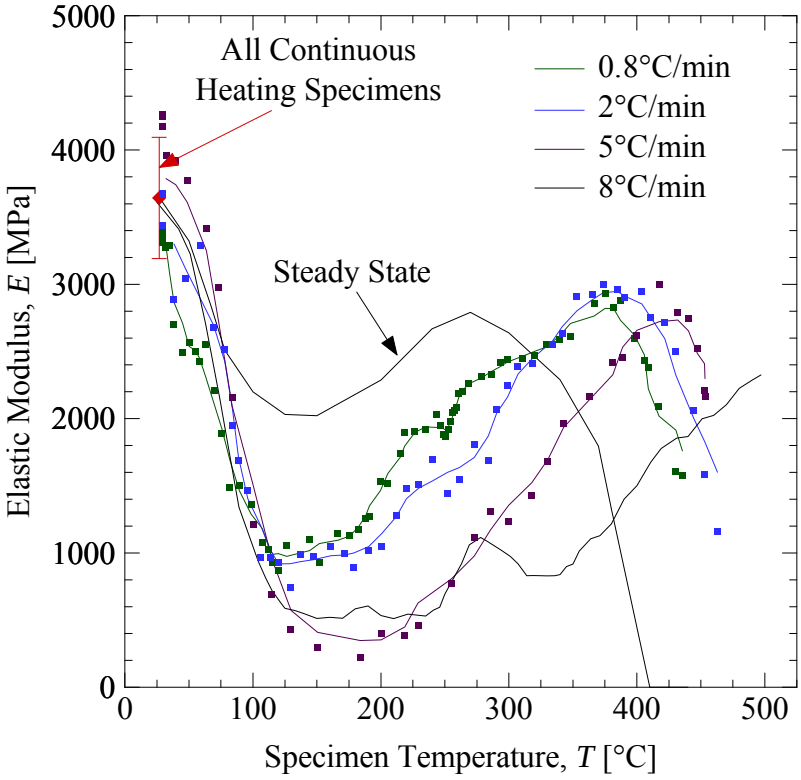

Figure 42: Comparison of the elastic modulus variation with temperature for specimens heated at 0.8, 2, 5, and 8°C/min along with the steady state data.

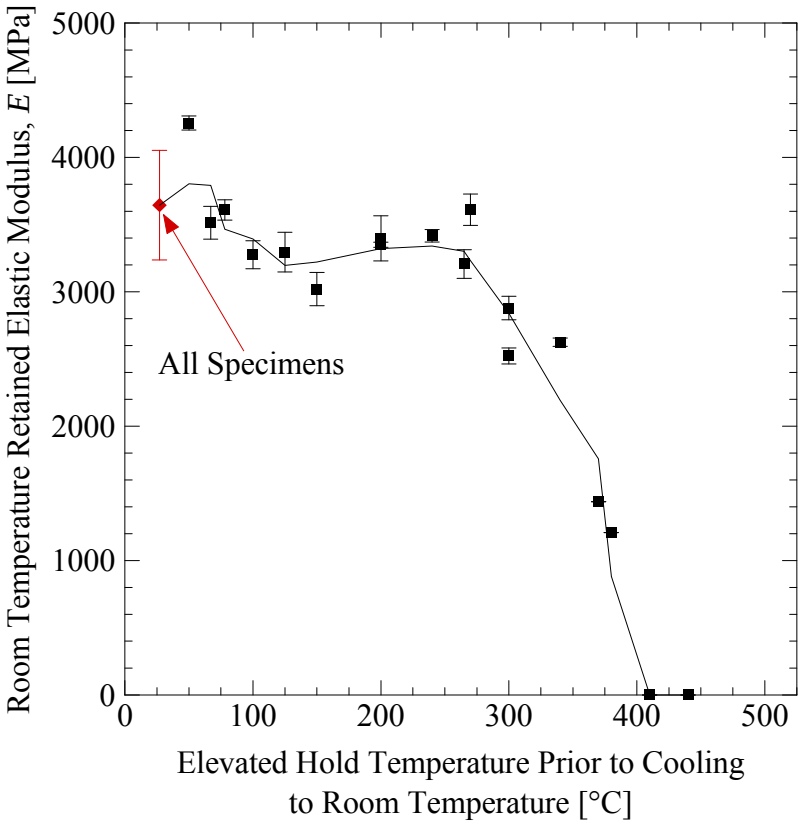

Figure 43: Retained room temperature elastic modulus as a function of the hold temperature prior to cooling with a moving average trend line.

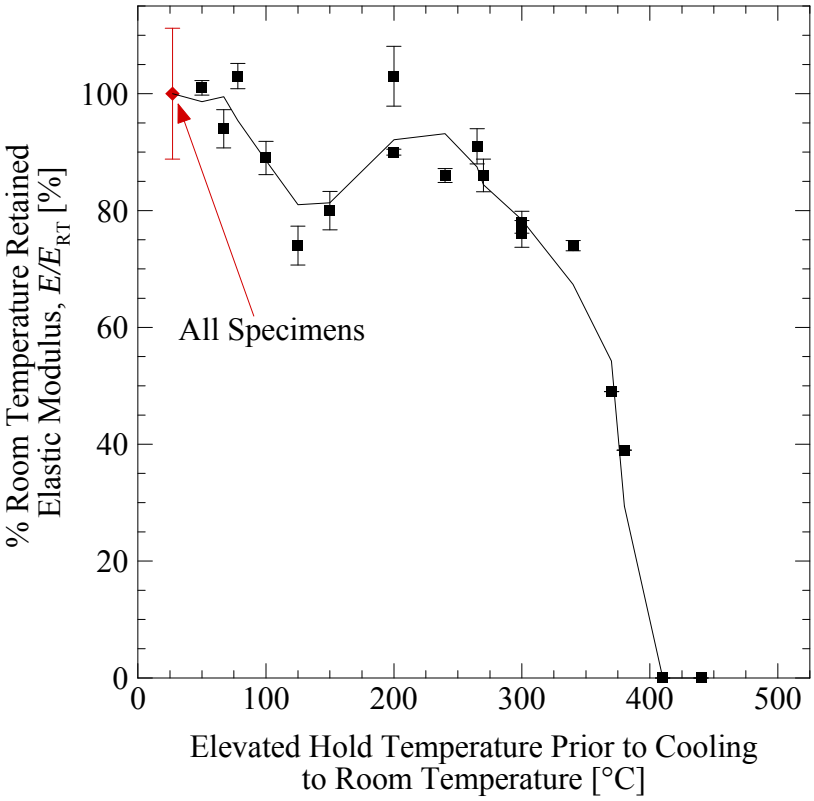

Figure 44: Retained room temperature elastic modulus percentage of specimens' initial room temperature elastic modulus as a function of the hold temperature prior to cooling with a moving average trend line.

CHAPTER 5. CONCLUSIONS

The present three-point bend elastic modulus measurements for PUNB bonded sand reveal a complex behavior during heating and cooling. Previous studies have only reported the room temperature or steady-state elastic moduli after extended holding of the bonded sand at elevated temperatures. The present measurements indicate that, for temperatures above 125°C, the variation of the elastic modulus with temperature is a strong function of the heating rate. Upon cooling, the permanent degradation of the binder prevents the bonded sand from regaining its original stiffness. The elastic modulus however appears to be independent of black iron oxide additive. This makes sense since the amount of binder in the system did not change with the addition of black iron oxide because binder was added as a function of total weight and not sand weight.

Before the present data can be used in stress simulations of a casting process, additional experiments are needed for more heating and cooling rates. In particular, the variations in the elastic modulus for the high heating rates that occur within 1 in of the mold-metal interface (> 50°C/min) have not at all been investigated in the present study. Measurements at such high heating rates are not possible using the present experimental setup because the oven is not capable of achieving such heating rates and the specimen temperature would be highly non-uniform. It is possible that ultrasonic, indentation, or other unconventional techniques for the measurement of the elastic modulus are suitable for bonded sand heated at high rates.

Another area of focus for future study is the effect of strain rate and plastic deformation. Due to the strong dependency on temperature and heating rate, this study did not investigate the effects of strain rate dependency. A compression test would be best suited since Wallace [4] reports a large difference in the yield stress at room temperature compared to bending or tension and the mold is predominantly under compressive stress. The current oven and set-up can not readily accommodate a

compression test due to the high loads necessary to strain a specimen sufficiently. A quick calculation using room temperature data suggests a 1,000 lb load cell would be required in order to test a specimen of sufficient size. Since the oven is not designed to work with available tension/compression testing machines, it was decided to focus sole on bend tests.

The current three point bend test could be used to measure the elastic modulus as a function of sand type, sand shape, grain fineness, binder level, and binder ratio. The complexity and amount of data needed to accurately predict the mechanical properties is far greater than one study can provide. The focus of this research was to better understand the behavior of the elastic modulus and the evolution under different heating conditions. Having done this, future tests can be tailored to investigate specific heating ranges and stress conditions.

REFERENCES

1. Monroe, C.A., Beckermann, C., and Klinkhammer, J., "Simulation of Deformation and Hot Tear Formation Using a Visco-Plastic Model with Damage," in Modeling of Casting, Welding, and Advanced Solidification Processes - XII, Eds. S.L. Cockcroft and D.M. Maijer, TMS, Warrendale, PA, 2009, pp. 313-320.

2. R.L. Naro and J.F. Hart, "Phenolic Urethane No-Bake Binders: Ten Years of Progress," *AFS Transactions*, vol. 88, 1980, pp 57-66.

3. D.F. Hoyt, "Identifying and Eliminating the Variables that Affect the Performance of Nobake and Coldbox Binder Systems," *AFS Transactions*, vol. 115, 2007.

4. P.J. Ahearn, F. Quigley, J.I. Bluhm, and J.F. Wallace, "Some Considerations On The Tensile And Transverse Strength Testing Of Shell Mold And Core Sands," *AFS Transactions*, vol. 64, 1956, pp. 125-132.

5. F. Quigley, P.J. Ahearn, and J.F. Wallace, "Influence Of Various Bonding Materials On Stress-Strain Characteristics Of Bonded Sands," *AFS Transactions*, vol. 65, 1957, pp 319-322.

6. N.Y. Huang and C.E. Mobley, "Mechanical Properties and Fracture Characteristics of Resin-Bonded Sands," *AFS Transactions*, vol. 91, 1983, pp. 751-764.

7. "Final Report," Arbeitsgemeinschaft Industrieller Forschungsvereinigungen Otto von Guericke, e.V. (AiF), 2008.

8. J. Thiel, "High Temperature Physical Properties of Chemically Bonded Sands Provide Insight into Core Distortion," Proc. 62nd SFSA Technical and Operating Conference, Chicago, Illinois, December 2008.

9. ASTM Standard C1211, 2002 (2008), "Standard Test Method for Flexural Strength of Advanced Ceramics at Elevated Temperatures," ASTM International, West Conshohocken, PA, 2008, DOI: 10.1520/C1211-02R08, www.astm.org.

10. Baratta, F.I., "Requirements for Flexure Testing of Brittle Materials," *Methods for Assessing the Structural Reliability of Brittle Materials, ASTM STP 844*, S.W. Freiman and C.M. Hudson, Eds., American Society for Testing and Materials, Philadelphia, 1984, pp. 194-222.

11. D.E. Kline, "A Recording Apparatus for Measuring the Dynamic Mechanical Properties of Polymers," *Journal of Polymer Science*, vol. 22, 1956, pp. 449-454.

12. J.R. Jenness, Jr., and D.E. Kline, "Dynamic Mechanical Properties of Some Epoxy Matrix Composites," *Journal of Applied Polymer Science*, vol. 17, 1973, pp. 3391-3422.

13. O. Heybey and F.E. Karasz, "Experimental study of flexural vibrations in thick beams," *Journal of Applied Physics*, vol. 47, No. 7, pp 3252-3260, July 1976.

14. ASTM Standard D5934, 2002 “Standard Test Method for Determination of Modulus of Elasticity for Rigid and Semi-Rigid Plastic Specimens by Controlled Rate of Loading Using Three-Point Bending,” ASTM International, West Conshohocken, PA, 2002, DOI: 10.1520/D5934-02, www.astm.org.

15. Y. Sakumoto, T. Nakazato, and A. Matsuzaki, “High-Temperature Properties of Stainless Steel for Building Structures,” *Journal of Structural Engineering*, vol. 122, n 4, pp. 399-406, April 1996.

16. S.R. Giese, S.C. Roorda, and M.A. Patterson, “Thermal Analysis of Phenolic Urethane Binder and Correlated Properties,” *AFS Transactions*, vol. 117, 2009, Paper# 09-112.